Titre: Title:	Design of a passive mechanism for machining purpose
Auteur: Author:	Hossein Heidariroshani
Date:	2013
Type:	Mémoire ou thèse / Dissertation or Thesis
Référence: Citation:	Heidariroshani, H. (2013). Design of a passive mechanism for machining purpose [Master's thesis, École Polytechnique de Montréal]. PolyPublie. https://publications.polymtl.ca/1098/

UNIVERSITÉ DE MONTRÉAL

DESIGN OF A PASSIVE MECHANISM FOR MACHINING PURPOSE

HOSSEIN HEIDARIROSHANI

DÉPARTEMENT DE GÉNIE MÉCANIQUE

ÉCOLE POLYTECHNIQUE DE MONTRÉAL

MÉMOIRE PRÉSENTÉ EN VUE DE L'OBTENTION

DU DIPLÔME DE MAÎTRISE ÈS SCIENCES APPLIQUÉES

(GÉNIE MÉCANIQUE)

AVRIL 2013

UNIVERSITÉ DE MONTRÉAL

ÉCOLE POLYTECHNIQUE DE MONTRÉAL

Ce mémoire intitulé:

DESIGN OF A PASSIVE MECHANISM FOR MACHINING PURPOSE

présenté par : HEIDARIROSHANI Hossein

en vue de l'obtention du diplôme de : Maîtrise ès sciences appliquées

a été dûment accepté par le jury d'examen constitué de :

M. MAYER René, Ph.D., président

M. BARON Luc, Ph.D., membre et directeur de recherche

M. BALAZINSKI Marek, Ph.D., membre

ACKNOWLEDGMENTS

I would like to thank my supervisor, Professor Luc Baron, for his precious time and effort, invaluable guidance and intellectual support in my graduate study.

Last but not least, I would like to thank the persons who directly or indirectly contributed to my thesis, but are not mentioned here.

ABSTRACT

This thesis presents a method of machining double curvature panels used in aeronautic industries. Normally, the machining of such panels is performed by chemical methods, yet given that chemical methods generate environmental problems, aeronautic industries have preferred the use of mechanical methods. During recent years, several mechanical methods have been proposed. Some of these methods use two devices which work synchronously; one is used to perform the machining, while the other is used as a support at the opposite side of the machining surface. This is known as the mince milling method or mirror milling.

This thesis proposes a compliant mechanism system allowing to machine aeronautic panels without requiring support at the opposite side of the surface. This mechanical system uses a 3-PSP topology with the cutting tool at its center. A compliant system is used for the orientation of the tool to maintain it normal to the surface to be machined.

The machining device is connected to the cutting surface by three sliding pads. The pads provide contact surfaces around the cutting tool to support the machining zone without requiring any support from the opposite side.

RÉSUMÉ

Ce mémoire présente une méthode d'usinage de panneaux double courbure utilisés dans les industries aéronautiques.

En général, l'usinage de tels panneaux est réalisé par des méthodes chimiques. Cependant, étant donné que les méthodes chimiques génèrent des problèmes environnementaux, les industries aéronautiques ont préféré l'utilisation de méthodes mécaniques. Au cours des dernières années, plusieurs méthodes mécaniques ont été proposées. Certaines de ces méthodes utilisent deux appareils qui fonctionnent de manière synchrone, l'un est utilisé pour effectuer l'usinage, tandis que l'autre est utilisé comme support sur le côté opposé de la surface d'usinage. Ceci est connu comme la méthode de ‹‹mirror milling››.

Ce mémoire propose un mécanisme passif permettant d'usiner les panneaux aéronautiques sans avoir besoin d'information précise sur la géométrie de la surface.

Ce mécanisme est composé de trois système majeurs :

Un mécanisme 3-PSP qui fournit l'orientation de l'outil de coupe sur la surface, système d'ajustement afin d'ajouter la profondeur de la coupe et un système de connexion qui sert à maintenir le contact entre l'outil de coupe et la surface.

TABLE OF CONTENT

LISTE OF TABLES

LISTE OF FIGURES

INTRODUCTION

The weight and fabrication cost of an aircraft have invariably been problematic for aircraft companies. However, nowadays, another arising issue is the undesirable ecological effect of aircraft fuel consumption. To resolve this problem, many companies have initiated new projects.

The fuel consumption of an aircraft is directly related to its weight. Therefore, reducing the weight of aircrafts may be a solution. One notable way of reducing aircraft weight is to eliminate the extra weight of various parts such as curved panels, also called fuselage panels. Nonetheless, due to its complexity, leading companies have launched new projects to facilitate machining methods which are less costly as well as eco-friendly.

The actual method for the machining of the curved panels was based on chemical machining. In this process, the aforementioned panels are first coated with a masking material to separate the untreated zones, thereby protecting them from chemicals and maintaining their thickness. In the second step the panels are immersed in a bath of chemicals whereby the unprotected zones of the panels are exposed to the chemicals and their masses are reduced. After several hours, the panel is taken out and washed. This process is performed repeatedly until the desired thickness of the machining zone is achieved.

Although this method allows a positional machining of the curved panels, there are significant drawbacks. First of all, the time and space required for this operation are considerable. Second, the recycling of the created sludge is complicated. For such reasons, several companies have decided to replace this method.

The technologies used for machining the fuselage panels mechanically instead of chemically were developed by the aerospace industry. Over the past few years, three main methods for mechanical machining of the fuselage panels have been documented.

Machine tool installation for supporting and machining workpieces

Figure 1, shows the machine tool installation for supporting the work piece [1]. This method involves the machine tool installation for supporting the work piece using a bed of hydraulic suction cups to support the machining work piece [1]. The system comprises multiple support columns grouped in modules by which the longitudinal movement of the support columns is

provided. These support columns can move in a transverse direction along the modules by means of a driving mechanism. At the upper end of each column there is a motor used to vertically drive the suction cups. All these movements are programmed by a computer, making the system fast and utterly automatic. The system can be used for machining a large number of panels with different forms used in the aerospace industry. This system is complemented by a portable machine carrying a multi-axis machining head above the panel. Due to the lack of rigidity between suction cups, this system is not useful for the machining of panels with a precision over 0.2 mm [2].

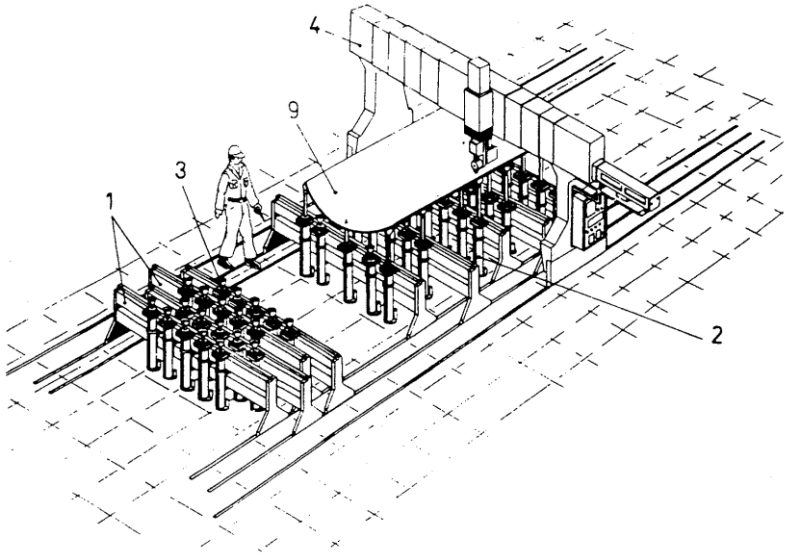

Figure 1: Machine tool installation for supporting and machining workpieces [1]

Process and device for machining by windowing of non-deformable thin panels

Figure 2, shows the Process and device for machining by windowing of non-deformable thin panels, proposed by Hamann. This method omits the bed of suction caps used in the first method and basically uses the isostatic positioning of the fuselage panels [2].

In this method, the isostatic positioning of the panels is obtained by placing two holes at the vicinity of two opposite edges as well as three contact points in order to eliminate the 6 degrees of freedom of the panel. Once in the isostatic position, the panel is held in position over the predetermined machining zone, named machining window, by using a programmed holding device. This mechanism is composed of multiple mobile and prehensile suction cups located towards the surface. The machining operation is carried out by using a multi-axis means at the

other side of the panel opposite the holding panel, and the holding device moves successively with regard to the machining window created on the panel.

According to this method, such panels are deformable and of low thickness. That is, they can be deformed under the machining force and even under their weight. However, the isostatic positioning of the panels is inadequate for suitable alignment of the panels and should be rigidified at more points.

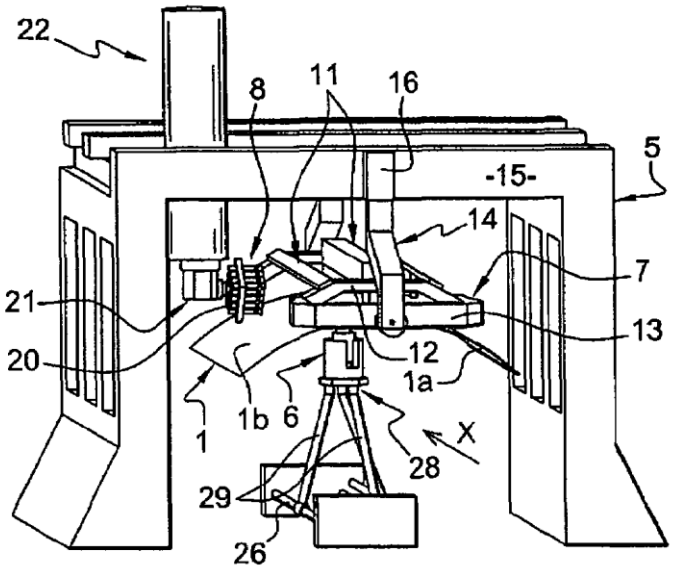

Figure 2 : Process and device for machining by windowing of non-deformable thin panels [2]

Mirror Milling

Figure 3, developed by [3] and [4], is a mechanical method of machining aircraft panels with a complex shape. This method uses a hyperstatic system by utilising a frame around the piece to be machined instead of using an isostatic system. Once the panel is held fixed on the periphery of a rigid support, a machining tool which is controlled numerically and adapted for multi-axial mobility is applied against the machining zone or the machining window. In order to support the machining zone, a mobile means is applied on the first surface of the panel opposite the other surface against the machining head. This mobile means is based on a mirror system with the machining tool and is controlled in permanent contact with the panel. This permanent application of the supporting means also precisely controls the thickness of the machined zone.

The Green panel project has developed a machine capable of machining these panels without using chemical methods. This method uses two machines working together based on the mirror system. Nonetheless, despite its advantages the fabrication costs are high. Therefore, the objective of this thesis is to design a mechanical system allowing to machine thin and large panels which is more versatile and inexpensive compared to the existing methods.

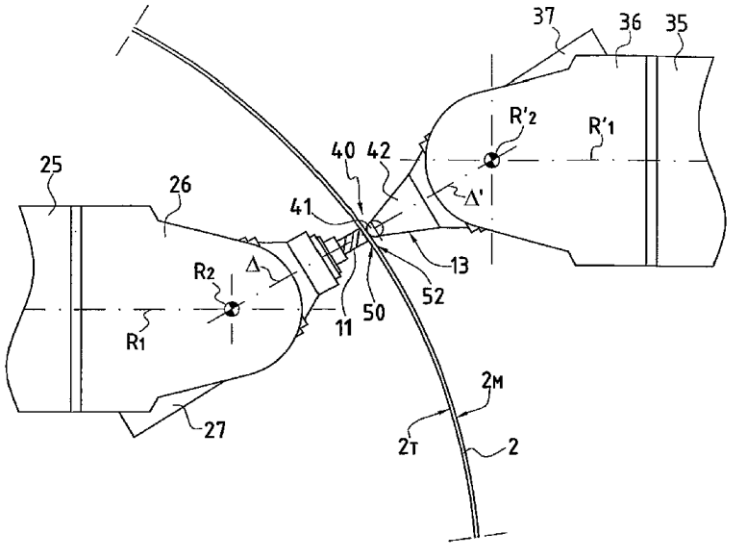

Figure 3 : Mirror Milling [4]

This thesis presents a new mechanical method for machining these panels by using the 3-DOF spatial compliant mechanism (two orientations and one translation). This mechanism is used for the orientation of the cutting tool as well as to maintain the tool normal to the cutting surface during the machining operation.

CHAPITRE 1 PROBLEM DEFINITION

Some aeronautic panels are thinning on certain location by a chemical processes. Thus, large panels must be machined on these panels with medium accuracy of location and high accurate remaining floor thickness. The overall machining time needs to be efficiently short to achieve good time efficiency. According to the documentation of the project the dimension of the thin panels are 0.1'' × 96'' × 170'' and the tolerance of the remaining floor thickness during machining is ± /0.002 po. We have, therefore, to design a mechanical system allowing to machine thin and large panels.

As mentioned in the introduction, mirror milling, although costly, is an alternative to chemical methods which uses a machine machining from one side and supporting the machining area from the other side.

1.1 General objective:

In this thesis our objective is to design a mechanism which is able to mount on a wrist of a robot providing the orientation of the cutting tool over the surface without requiring precise information about the geometry of the surface.

1.2 Specific requirements:

A mechanism which provides the orientation of the cutting tool according to the geometry of the surface and maintains the cutting tool normal to the surface.

1- Design of a passive 3-DOF (three degrees of freedom) spatial parallel mechanism having two orientations and one passive translational degree of freedom.

2- Using a passive element such as spring in the mechanism thereby providing the compliant motion of mechanism as the mechanism moves over the surface.

3- Design mechanism of three sliding pads in order to maintain contact between the cutting tool and surface.

CHAPITRE 2 LITERATURE REVIEW

In many industrial tasks the parallel mechanisms with less than 6-DOF is more considered. Among these less than 6-DOF mechanisms, the 3-DOF remains an important group due to their application in many industries. For example, in machining, measuring machines or in spherical wrist of the serial mechanisms as well as many other applications [5].

Among the 3-DOF mechanisms, the zero-torsion parallel mechanism, having two orientations and one translational degree of freedom, (3-DOF) is the most preferred for the machining of thin aeronautical panels [18]. Given that the designed mechanism in this thesis belongs to this group of mechanisms, the purpose of this chapter is to present the classification of existing 3-DOF parallel mechanisms along with their applications and compare their advantages and disadvantages.

2.1 Basic Terminology

Mechanism*:* System of bodies designed to convert motions of, and forces on, one or several bodies into constrained motions of, and forces on, other bodies [21].

Kinematic chain: Assemblage of links and joints [21].

Serial mechanisms

A serial mechanism is an open-loop mechanism composed of a group of rigid links connected to different types of joints (revolute, prismatic, etc.). In serial mechanisms, the first link is the base and is fixed to the ground, and the last link is the output link and can move in the space [6].

“Open kinematic chains are usually described by the sequence of their kinematic pairs (joints), where the following notation is used for the kinematic pairs:

P: prismatic; R: revolute; U: universal; S: spherical” [21].

There are some advantages to this type of mechanism such as large work space and high dexterity. Nevertheless, they suffer from disadvantages such as low precision due to cumulative joint errors, deflection of the links, poor force extension capability, low payload-to-weight ratio due to cumulative weight of the successive links on every actuator and high inertia because of numerous moving links that form a long beam.

Parallel mechanisms

"Closed-loop mechanism in which the end-effector (mobile platform) is connected to the base by at least two independent kinematic chains. Parallel mechanisms with identical kinematic chains are denoted as *n-JJJJ* where *n* is the number of kinematic chains, and *JJJJ* denotes the type of kinematic chain, with the last letter denoting the kinematic pair at the mobile platform" [21].

There are several advantages and disadvantages of parallel mechanisms. Their advantages are high stiffness, high payload-to-weight ratio due to load sharing of several limbs, high accuracy due to no cumulative joint error and low inertia of moving parts. The disadvantages are low work space, low dexterity and a complicated direct kinematic solution.

2.2 3-DOF Parallel Mechanisms

Parallel mechanisms (PMs) with less than six degrees of freedom have been the attracted subject in the academy and industry research since the majority of manipulation tasks only need 3DOF.

According to the type of platform motion, the 3-DOF parallel mechanism can be classified into the following four categories [5]:

(i) planar mechanisms, (ii) translational mechanisms, (iii) rotational or spherical mechanisms and (iv) mixed-motion mechanisms.

2.2.1 3-DOF Planar Mechanisms

These are mechanisms in a plane consisting of a moving platform with three degrees of freedom such that two of them are translations along the x and y axis and the third one is a rotation about the z-axis. Hence, a 3-DOF planar mechanism has three independent kinematic chains actuated by three actuators [7].

Each chain is composed of two rigid bodies connected to each other by three prismatic or revolute joints of which one is actuated and two are passive. Each serial chain is connected to the base and to the moving platform at its two ends and can be described by the joint sequence connecting the rigid bodies from the base to the platform. The serial chains can be presented in the following form: RRR, RPR, RRP, RPP, PRR, PPR, PRP, and PPP.

Figure 2-1 shows the different fully parallel planar mechanisms with three degrees of freedom and identical chains. It must be mentioned that the PPP chain is similar to the PRP chain.

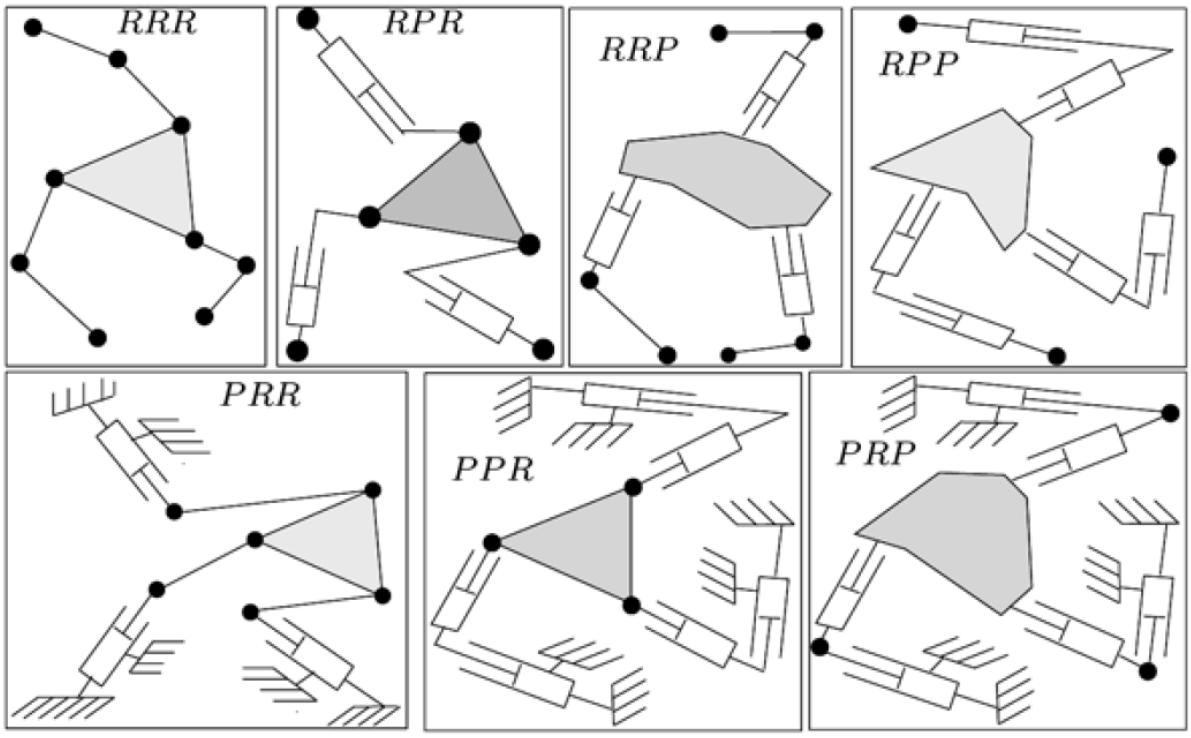

Figure 2-1 : The different fully parallel planar mechanisms with three degrees of freedom and identical chains [7].

2.2.2 3-DOF Spatial Mechanisms

a) Translation Mechanisms

A translational parallel mechanism has three degrees of freedom all of which are translational. These mechanisms can be used in assembly and machining operations.

They consist of a platform and connecting chains in parallel configuration between the base and platform. The applicable joint types in this kind of mechanism are revolute, prismatic, universal and spherical [8].

First, a translational parallel mechanism composed of three identical limbs which consists of two links and three joints is considered. Table 2-1 illustrates the feasible kinds of limbs categorized into two types [8].

Table 2-1 : Feasible limb configuration for 3-DOF spatial mechanisms [8]

Type	Kind
201	RRS, RSR, RPS, RSP, PSR, PRS, SPR, PPS, PSP, SPP
120	UPU, RUU, PUU

The first, second and third digits in Table 2-1 represent the number of joints with one, two and three degrees of freedom, respectively. Hence, type 201 indicates two one-DOF, zero two-DOF and one three-DOF joints in each limb and type 120 represents one one-DOF, two two-DOF and zero three-DOF joints in each limb. All joints in each limb are directed left to right indicating the joint connected from the base, the intermediate joint and the joint connected to the platform, respectively.

Since it is preferable that the ground-connected joint for the actuation purpose be a revolute or prismatic joint, or an intermediate prismatic joint, SRR, SRP, URU, UUR and UUP limb configurations can be neglected. Each limb should constrain a rotational degree of freedom. Therefore, the rotation of the moving platform is completely eliminated by the total constraints of the three limbs in order to have pure translational motion for the mechanism. Since the spherical joint cannot constraint any rotation of the mechanism, all the limb configurations including the spherical joint should be eliminated. The three feasible limb configurations for this kind of mechanism are UPU, RUU and PUU.

Figures 2-2, 2-3 and 2-4 show the schematic diagrams of configurations 3-UPU, 3-PUU and 3-RUU. The kinematics of the 3-UPU mechanism has been studied in [22].

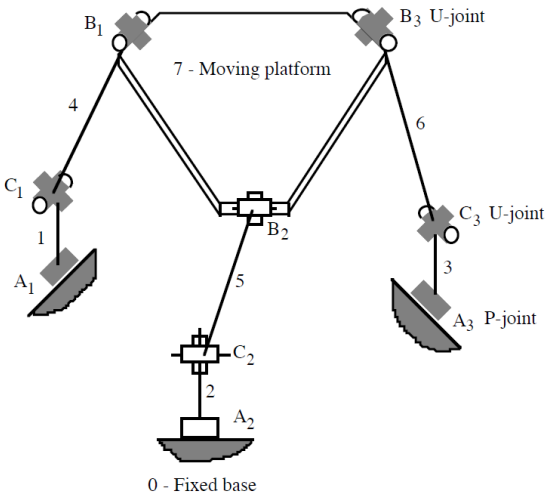

Figure 2-2 : A spatial three-DOF, 3-UPU translational platform [8]

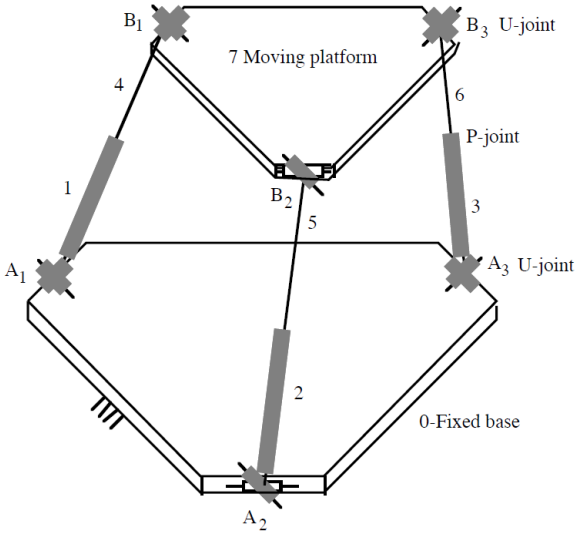

Figure 2-3 : A spatial three-DOF, 3-PUU translational platform [8]

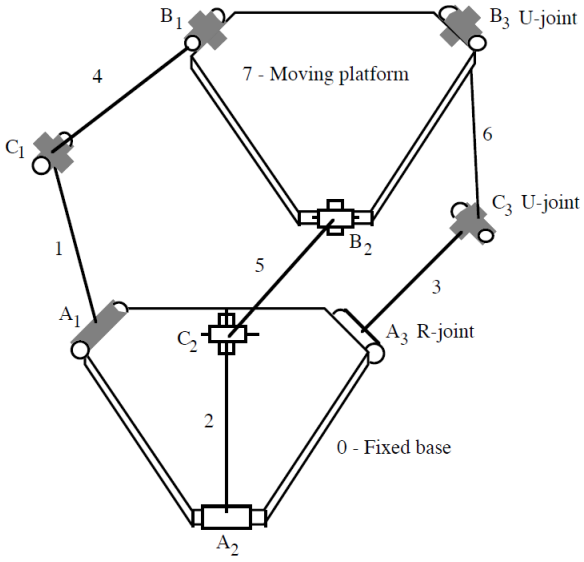

Figure 2-4 : A spatial three-DOF, 3-RUU translational platform [8]

b) Orientation Mechanisms

An orientation or spherical parallel mechanism has three degrees of freedom and its motion controls only the orientation of the platform without varying the platform position [9].

Applications of this kind include orientation of machine tool beds and workpieces, solar panels, etc.

Figures 2-5 – 2-10 show several existing rotational parallel mechanisms such as 3-UPU, 3-RUU, 3-RSS, 3-CRU, 3-UPC and 3-CRC.

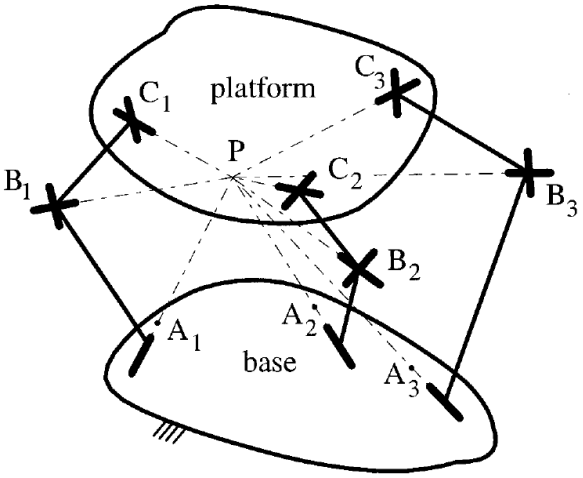

Figure 2-5 : 3-RUU wrist [10]

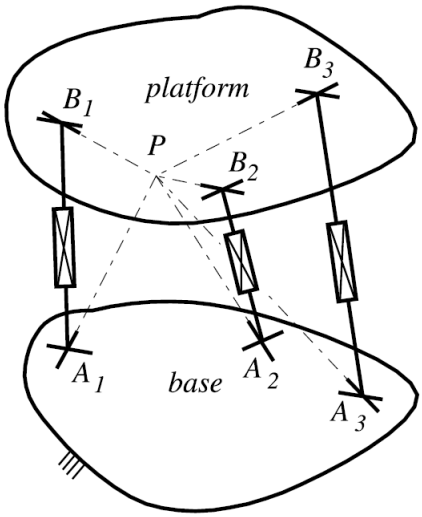

Figure 2-6 : 3-UPU rotational mechanism [11]

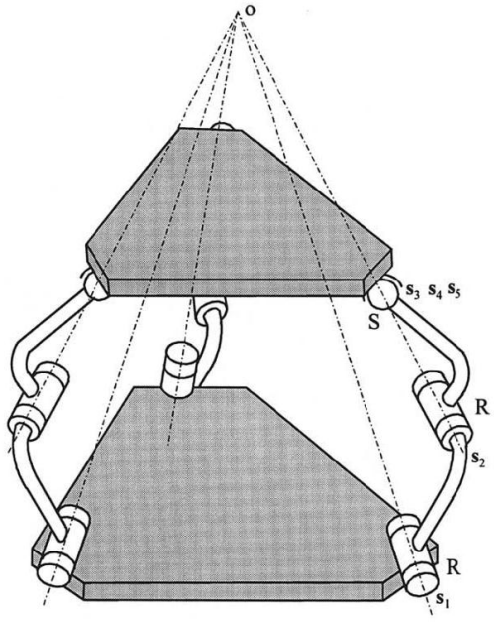

Figure 2-7 : A 3-RRS rotational parallel mechanism [12]

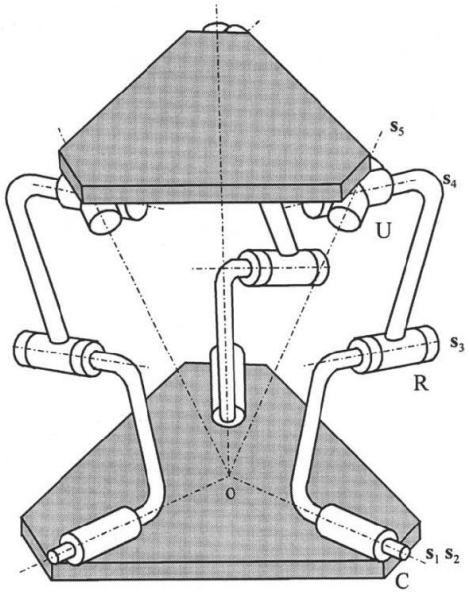

Figure 2-8 : A 3-CRU rotational parallel mechanism [12]

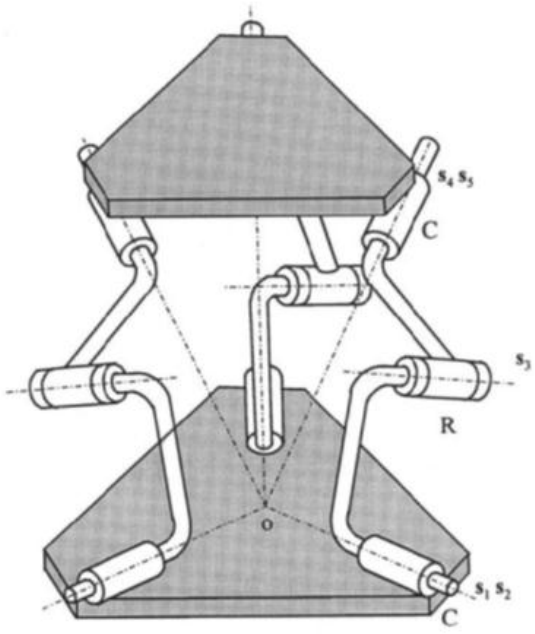

Figure 2-9 : A 3-CRC rotational parallel mechanism [12]

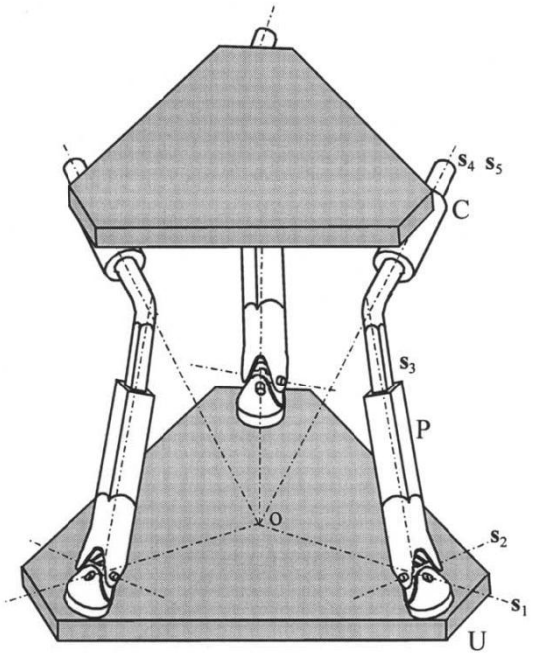

Figure 2-10 : A 3-UPC rotational parallel mechanism [12]

c) Mixed Degrees of Freedom Mechanisms

This is a kind of mechanism in which the motion of the platform is not limited by pure translation or pure rotation yet rather a combination of translation and rotation [5].

2.3 The Tilt-and-Torsion Angles

"The use of tilt-and-torsion angles provides the fittest tool for geometric analysis of parallel mechanism, especially for the zero torsion parallel mechanisms" [13]. Since our designed mechanism belongs to the zero-torsion mechanisms, we will use this concept for the kinematic analysis of the designed mechanism.

Generally, three rotations about the coordinate axes can give the body an arbitrary orientation in space. These rotation angles are called Euler angles [13]. As the orientation of the body in space changes, the coordinate transformation associated with this change can be described through a 3×3 proper orthogonal matrix named $\boldsymbol{Q}$.

Two coordinate systems, namely A={X, Y, Z} and B= $\{x, y, z\}$ are considered to be the fixed frame (base) and the mobile frame, respectively. **P** and $\acute{\mathbf{P}}$ are the position vectors of a point expressed in

A and B, respectively, and $\boldsymbol{Q}$ is the rotation matrix that carries frame A into a new attitude, that of frame B. The coordinate frame associated with this orientation change is defined by a 3×3 orthogonal rotation matrix,

$$\mathbf{P} = \boldsymbol{Q}\acute{\mathbf{P}}$$

$\boldsymbol{Q}$ represents a rotation with an angle $\emptyset$ around an axis. Then any $\boldsymbol{Q}$ can be described by the multiplication of three rotations.

$$\boldsymbol{Q}_x(\emptyset_x) = \begin{bmatrix} 1 & 0 & 0 \\ 0 & \cos\emptyset & -\sin\emptyset \\ 0 & \sin\emptyset & \cos\emptyset \end{bmatrix},\ \mathbf{Q}_y(\emptyset_y) = \begin{bmatrix} \cos\emptyset & 0 & \sin\emptyset \\ 0 & 1 & 0 \\ -\sin\emptyset & 0 & \cos\emptyset \end{bmatrix},\ \boldsymbol{Q}_z(\emptyset_z) = \begin{bmatrix} \cos\emptyset & -\sin\emptyset & 0 \\ \sin\emptyset & \cos\emptyset & 0 \\ 0 & 0 & 1 \end{bmatrix}$$

Since order is important in matrix multiplication, twelve sequences of $\boldsymbol{Q}$ can be identified as follows: XYZ, XZY, YXZ, YZX, ZXY, ZYX, XYX, XZX, YXY, YZY, ZXZ, ZYZ. Using the ZYZ sequence, $\boldsymbol{Q}$ will be $\boldsymbol{Q} = \boldsymbol{Q}_x(\emptyset_x)\boldsymbol{Q}_y(\emptyset_y)\boldsymbol{Q}_z(\emptyset_z)$

Generally, different sequences are used in different fields. For example, in physics textbooks, the sequence used is ZXZ and the three rotation angles are referred to as precession, nutation and spin. In the automotive and machine tool industries, the term more commonly used is XYZ and the rotation angles are named roll, pitch, and yaw.

Figure 2-11 illustrates the three rotations in the ZYZ system. The three rotations are performed as follows:

- Rotate the XYZ system about the Z-axis by $\emptyset$. The x-axis is now at angle $\emptyset$ with respect to the X-axis and y-axis is now at angle $\emptyset$ with respect to the Y-axis.
- Rotate the XYZ-system again about the y-axis by θ. The z-axis is now at angle θ with respect to the Z-axis.
- Rotate the XYZ system a third time about the z-axis by ψ. The x^*-axis is now at angle ψ with respect to the x-axis and the y^*-axis is now at angle ψ with respect to the y-axis. The first and third axes are identical.

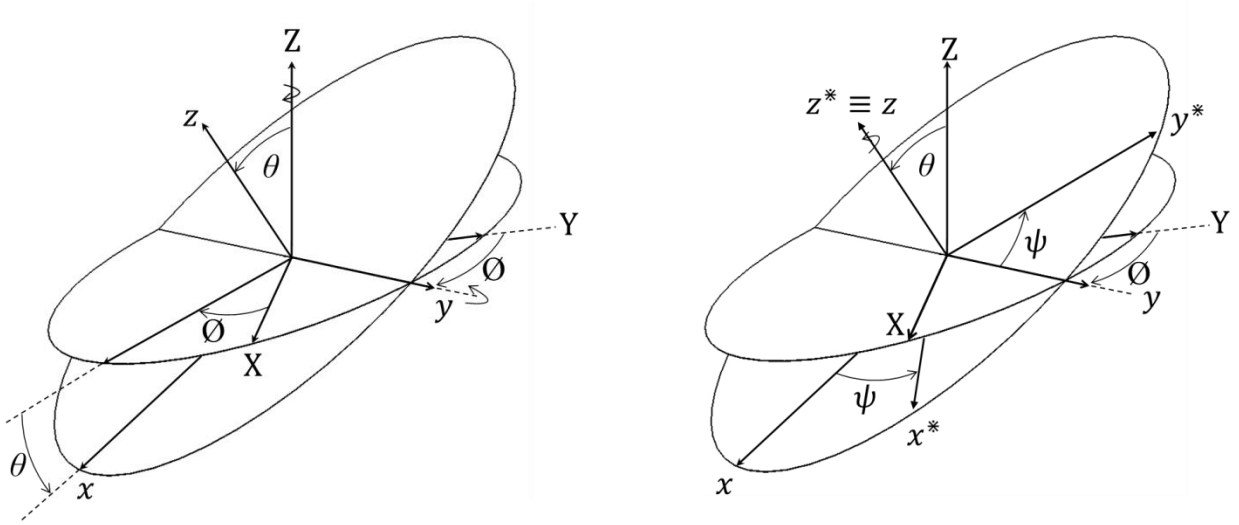

Figure 2-11 : The ZYZ rotation system: Pecession, nutation and spin [13]

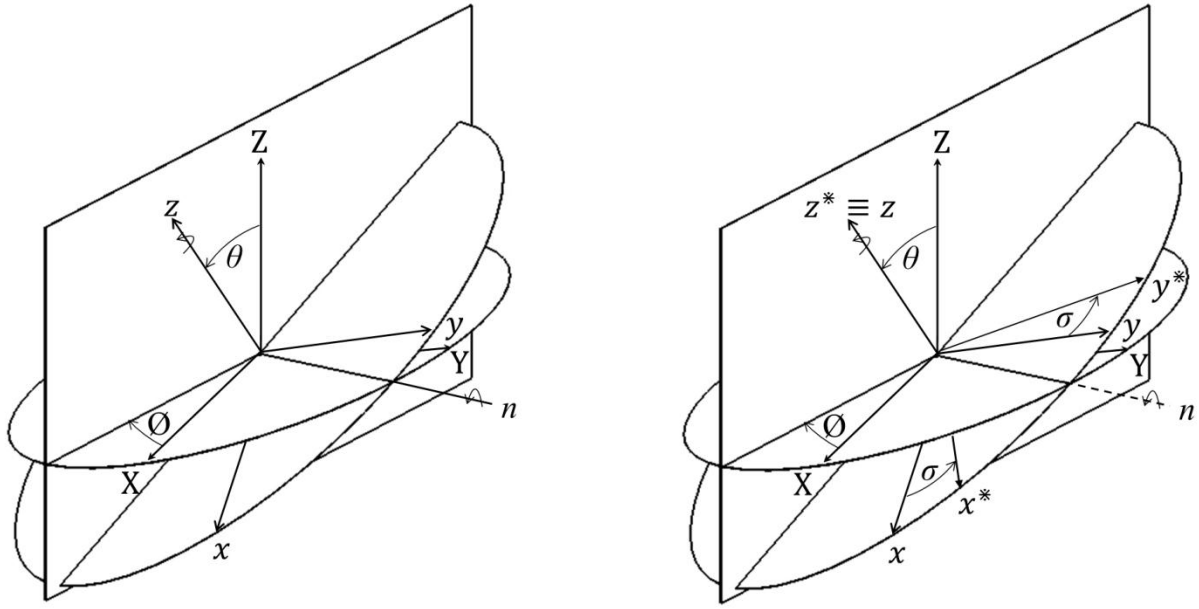

Figure 2-12 : The T&T rotations: tilt and torsion angles [13]

As it can be seen from the Fig. 2-12, in the first step (precession and nutation), the Z-axis coincides with the new attitude and is then spun to its final position. The main objective in the first two steps is to bring the Z-axis to its new position. It can be achieved by a single rotation about the variable horizontal axis *n* named tilt axis and the resulting angle is referred to as a tilt angle.

When the body reaches its final position directly by rotating about the tilt axis, it means that the precession and nutation in the ZYZ system is performed only by a single rotation in the new system. Therefore, only the final sequence of orientation (spin) remains in order to complete the full rotation of the body. As shown in Fig. 2-12, in the new system, the last orientation is not the same as spin in the ZYZ system. Hence a different name and notation should be used; the name and notation used are torsion and (σ) respectively.

In this system, instead of three coordinate-axis rotations $\boldsymbol{Q} = \boldsymbol{Q}_z(\emptyset)\boldsymbol{Q}_y(\theta)\boldsymbol{Q}_z(\psi)$, there are just two rotations $\boldsymbol{Q} = \boldsymbol{Q}_n(\theta)\boldsymbol{Q}_z(\sigma)$ where $\boldsymbol{Q}_n(\theta) = \boldsymbol{Q}_z(\emptyset)\boldsymbol{Q}_y(\theta)$ and $\boldsymbol{Q}_n(\theta) = \boldsymbol{Q}_z(\emptyset)\boldsymbol{Q}_y(\theta)\boldsymbol{Q}_z(-\emptyset)$. This indicates that after completing precession and nutation, a $(-\emptyset)$ is needed to spin back in order to complete the rotation [13]. Therefore

$$\boldsymbol{Q} = \boldsymbol{Q}_n(\theta)\boldsymbol{Q}_z(\sigma) = \boldsymbol{Q}_n(\theta) = \boldsymbol{Q}_z(\emptyset)\boldsymbol{Q}_y(\theta)\boldsymbol{Q}_z(-\emptyset)\boldsymbol{Q}_z(\sigma) = \boldsymbol{Q}_z(\emptyset)\boldsymbol{Q}_y(\theta)\boldsymbol{Q}_z(\sigma - \emptyset)$$

and

$$\boldsymbol{Q} = \begin{bmatrix} \cos^2\emptyset\cos\theta + \sin^2\emptyset & \sin\emptyset\cos\emptyset(\cos\theta - 1) & \cos\emptyset\sin\theta \\ \sin\emptyset\cos\emptyset(\cos\theta - 1) & \sin^2\emptyset\cos\theta + \cos^2\emptyset & \sin\emptyset\sin\theta \\ -\sin\theta\cos\emptyset & -\sin\theta\sin\emptyset & \cos\theta \end{bmatrix}$$

2.4 Zero-Torsion 3-DOF Spatial Mechanisms

In various parallel mechanisms, the rotational degree of freedom about the z-axis is irrelevant, e.g. in a mechanism which is equipped with an axisymmetric rotating milling tool along its z-axis.

Some parallel mechanisms have three identical legs. In the majority of these parallel mechanisms, the platform motion consists of one translation and two rotations. In many cases, the orientations are such that the torsion is zero. Three main examples of zero torsion mechanism with three identical legs are 3-RSR, 3-PPS and 3-PSP.

2.4.1 3-RSR 3-DOF Spatial Mechanisms

One unit of the mixed-orientation PM family is the mechanism with a 3-RSR topology. In this mechanism, the platform is connected to the base frame through three RSR serial chains (revolute, spherical and revolute joints).

Depending on its structure, the mechanism can be either spherical or mixed-motion [5]. It is of the spherical type when all the revolute joint's axes intersect at a common point as in Fig. 2-13. It is said to be the mixed type if the three revolute joint's axes are coplanar as in Fig. 2-14. Bonev studied the constraint analysis of this mechanism [13] as shown in Fig. 2-15.

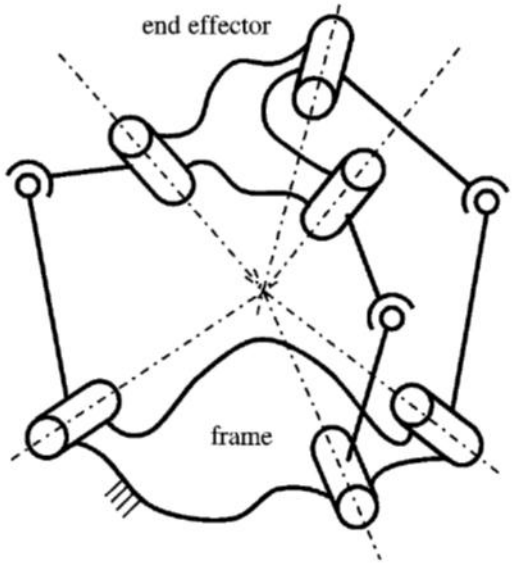

Figure 2-13 : The 3-RSR wrist [5]

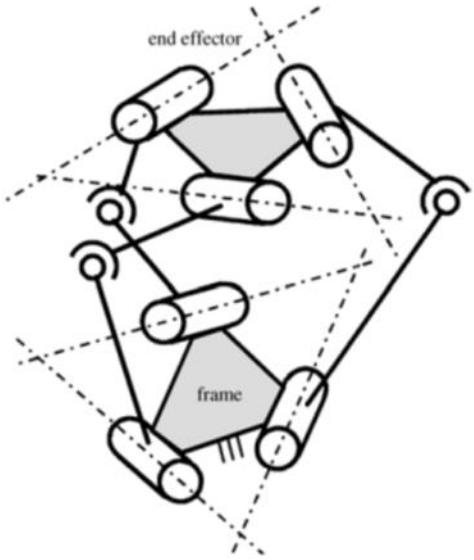

Figure 2-14 : Dunlop and Jones' 3-DOF RSR mechanism [5]

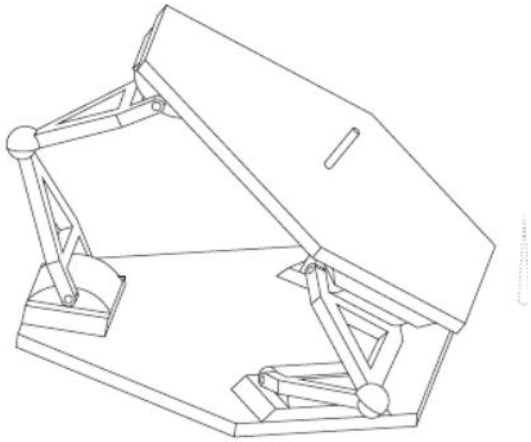

Figure 2-15 : A 3-RSR 3-DOF spatial symmetrical parallel mechanism [13]

2.4.2 [PP]S 3-DOF Spatial Mechanisms

This mechanism belongs to the zero-torsion family with a topology of 3-PRS capable of performing 3-DOF motion, two orientations and one translational degree of freedom. This mechanism consists of two platforms where one is movable and the other is fixed (namely base). They are connected through three identical limbs.

Each of these three limbs is formed by two fixed length links and three joints. The first joint is an actuated prismatic joint connecting the base frame and first link. The first link is again connected to the second link by means of a passive revolute joint and finally a spherical joint followed by a revolute joint connects the second link to the moving platform.

Three different configurations of this mechanism have been studied by different researchers as presented in Figs. 2-16, 2-17 and 2-18. The first model, shown in Fig. 2-16, was proposed for the first time by Carretero et al. [15] and the other two were proposed by Tsai et al [16] and Merlet [17], respectively. The 3-PRS model of Carretero et al. was used for orientation and positioning of a Cassegrain telescope as shown in Fig. 2-16 [14].

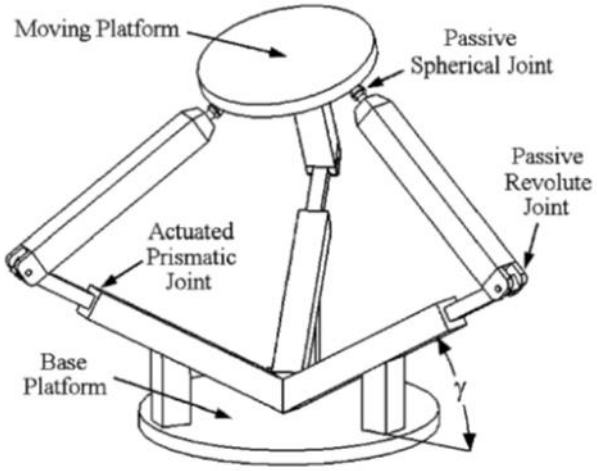

Figure 2-16 : Carretero et al.'s model of the 3-PRS the 3-PRS mechanism [14]

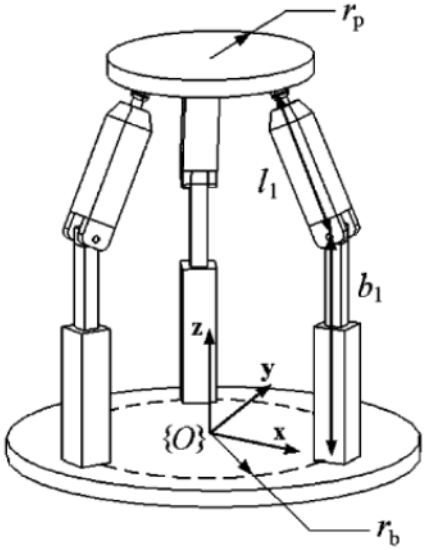

Figure 2-17 : Tsai et al.'s model of mechanism [14]

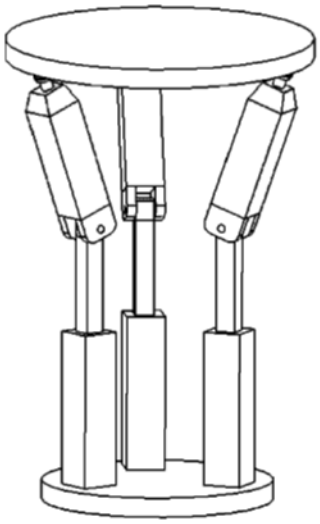

Figure 2-18 : Merlet's model of the 3-PRS mechanism [14]

In Carretero model, there is an inclination angle γ between the actuated prismatic joints and the base frame and the three axes of the prismatic joints intersect at a common point [14]. In the 3-PRS configurations proposed by Tsai and depicted in Fig. 2-17, the axis of the actuated prismatic joints are perpendicular to the base frame ($\gamma = 90^{\circ}$) and intersect the base frame at a radial distance r_b from the base platform [14]. This mechanism, as shown in Fig. 2-19, was proposed as a three-axis articulated tool head by Xin-Jun Liu, Li-Ping Wang, Fugui Xie and Ilian A. Bonev [18]. The third model of 3-PRS depicted in Fig. 2-18 was proposed by Merlet and used as an add-on device to the end of an endoscope in biopsy procedures [17].

The differences between these three configurations are studied in [14]. The main difference between the Carretero model and the others is that the translation along the *z*-axis is limited and hence the motion of the moving platform along this axis is finite. However, for other configurations, it is infinite due to the perpendicularity of the actuated prismatic joints. Therefore the main difference between the Tsai model and the other two models is that the work space volume of Tsai device is larger than the others.

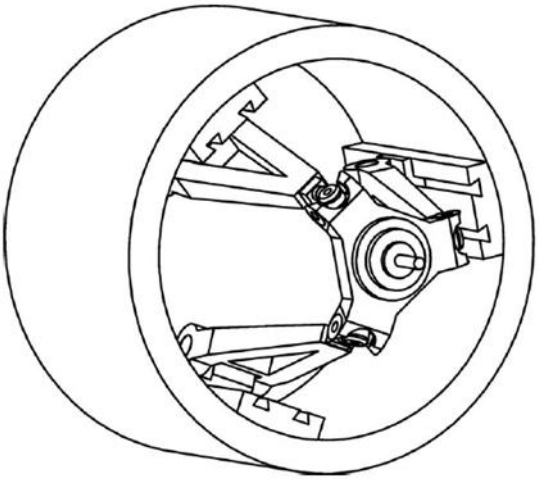

Figure 2-19 : Kinematic structure of a three axisarticulated tool head [18]

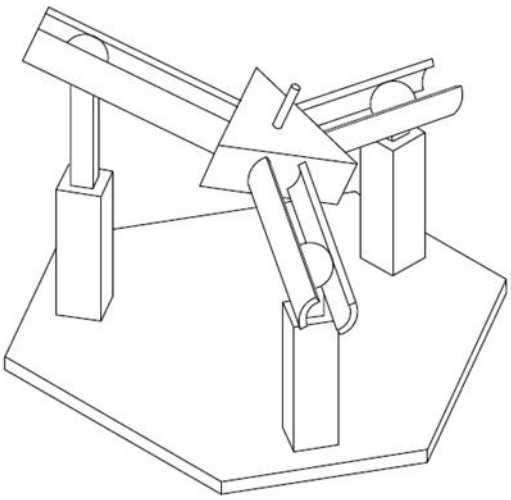

Figure 2-20 : 3-PSP mechanism [13]

2.4.3 3-PSP 3-DOF Spatial Mechanisms

As shown in Fig. 2-20 the tripode joint mechanism is a somewhat more complicated 3-DOF spatial parallel mechanism. This kind of mechanism is used in automotive industries and belongs to the class of 3-DOF zero torsion spatial parallel mechanisms [13]. It is composed of three PSP chains. Each limb contains two prismatics and one spherical joint. The first three prismatic axes are fixed at an 120° angle on the base frame and are parallel. The three spherical joints slide along these fixed axes and the three other prismatic axes intersect each other at 120° and are traced by the spherical joints. These prismatic axes, by which the platform is moved, are coplanar. We will use this mechanism to design our spatial mechanism used for the machining of curved panels.

2.5 Conclusion

In this thesis the target is to design a passive 3-DOF spatial parallel mechanism belonging to the group of zero-torsion mechanisms. This has a mechanism with two orientations and one passive translational degree of freedom which can be used for the machining of curved panels without requiring precise information about the geometry of the surface.

In the first step of this chapter the parallel and serial mechanisms have been presented and their advantages and disadvantages for the machining have been compared. Subsequently, the 3-DOF

parallel mechanisms were classified into two major groups of planar and spatial mechanisms. We chose the 3-DOF spatial mechanisms because the planar ones were not compatible for our design since we need two orientations and one passive translation degree of freedom.

From the 3-DOF spatial parallel mechanisms we introduced the translational, pure orientation and mixed orientation group of mechanisms. Next, we introduced zero-torsion spatial mechanisms which have two orientations and one translation degree of freedom and are most attracted for the manufacturing of thin panels. Then from this group, the three types of mechanisms with the kinematic chains of 3-RSR, 3-PRS and 3-PSP have been presented in detail. As mentioned, the 3-PRS mechanism is successfully used for high speed machining of aircraft components from aluminum alloy plate [18]. In this thesis, we chose the more complicated one, that is 3-SPS for the design of passive 3-DOF spatial parallel mechanism.

CHAPITRE 3 2-DOF PLANAR MECHANISM

As mentioned in chapter 1, our goal is to design a passive 3-DOF spatial mechanism used for the machining of curved panels. In this mechanism, the cutting tool is located at the center of the mechanism and has compliant motion in the direction parallel to the axis of the cutting tool with the use of 3 springs. The mechanism is placed on the machining surface and moves over it by using 3 contact points. This mechanism is designed in such a way that, the cutting tool is always in contact with the cutting surface through the contact points and can be aligned normally to the surface by using the 3-PSP system. In chapter 4 this mechanism will be presented in detail.

Before studying this spatial mechanism, let us study its planar first counterpart, i.e., a passive planar 2-DOF mechanism used to maintain the tool axes normal to a curve. This simpler mechanism uses a similar concept, but it is considered to be in the plane since it is the planar mechanism, therefore the wavy surface is assumed to be the curve on the plane. This mechanism is fixed to the base frame and rotates about its origin. In this mechanism, the cutting tool is placed at the symmetry axis of the mechanism and has the compliant motion in the direction parallel to the axis of the cutting tool by using a spring. Mechanism is connected to curve through two contact points. As the curve moves in the direction parallel to the horizontal axis, the mechanism rotates about the origin of the base frame and aligns the cutting tool normal to the curve.

The objective of presenting this design is to verify the possibility of machining the curved surface using a compliant system with a planar mechanism. We will use this concept to design a passive spatial mechanism.

As shown in Fig. 3-1 this mechanism is designed to move on a curve by using two contact points and as it moves on the curve it changes the orientation of the tool and maintains the tool normal to the curve. In the first section the kinematic chain of the aforementioned mechanism is presented and then followed by how these parts relate to its kinematic analysis in the 1-DOF and 2-DOF cases.

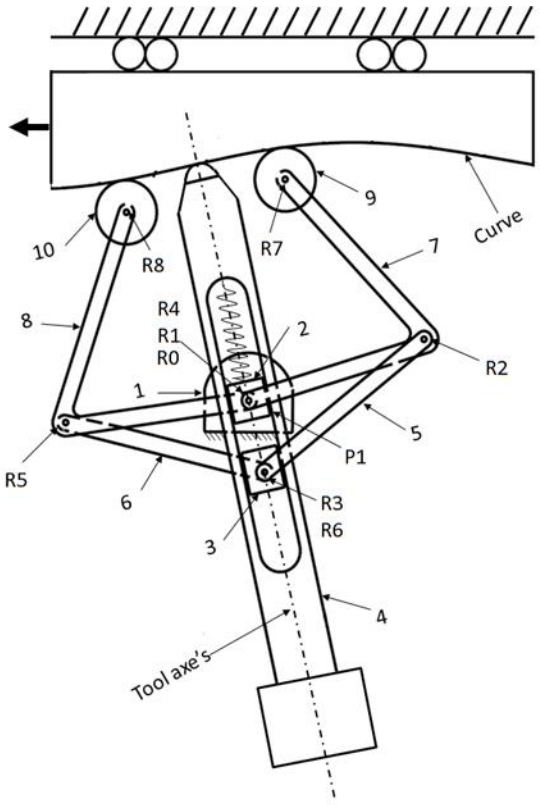

Figure 3-1 : Schematic of the 2-DOF planar mechanism

Table 3-1 : Link identification

No.	Link name
1	*Base Link*
2	*Slider A*
3	*Slider B*
4	*Tool*
5	*Link A*
6	*Link B*
7	*V-Link A*
8	*V-Link B*
9	*Roller A*
10	*Roller B*

Table 3-2 : Joint identification

Joint	Link connection
R0	Revolute joint between links 1 & 2
R1	Revolute joint between links 7 & 2
R2	Revolute joint between links 7 & 5
R3	Revolute joint between links 4 & 6
R4	Revolute joint between links 8 & 2
R5	Revolute joint between links 8 & 6
R6	Revolute joint between links 8 & 6
R7	Revolute joint between links 7 & 9
R8	Revolute joint between links 8 & 10
P1	Prismatic joint between links 2 & 4

Figure 3-1 shows the schematic of this mechanism. The system consists of 10 links and two symmetric sides where the cutting tool is located along the axis of symmetry. These symmetric sides are connected to each other through two rigid links (*Slider A & Slider B*). One (*Slider A*) is attached to the origin of the base frame providing rotation of the cutting tool about the origin of the base frame, while the other link 3 (*Slider B*) is used to adjust the depth of cut and is fixed to the cutting tool during machining. The designed mechanism can align the tool at the symmetric axis, normal to the curve. A spring connects link 2 (*Slider A*) to link 4 (*Tool*) and provides the compliant motion of the tool. The stiffness of the spring by which the *Tool* is held is such that the *Tool* has compliant motion in the direction normal to the curve.

3.1 Kinematic Chain

Figure 3-2 shows the kinematic chain of the mechanism. The vertices are numbered from 1 to 8 representing links 1 to 8, the two rollers are numbered 9 and 10 and the joints are labelled as R and P.

Link 1 (*Base Link*) is considered to be the base. Link 2 (*Slider A*) is attached to the origin of the *Base Link* and has only one rotation about the origin (R0). This link causes the rotation of link 4 (*Tool*) about the origin of the *Base Link*. As mentioned, link 3 (*Slider B*) is used to adjust the depth of cut and during machining will be attached to link 4 (*Tool)*, therefore for the kinematic analysis of the mechanism they are considered to be one link, named *Tool*. Link 4 (*Tool*) has two movements, one rotation about the origin of the *Base Link* and one translation along its vertical axis. Link 5 (*Link A*) is a rigid link connected to link 7 (*V-Link A*) and link 4 (*Tool*) with two revolute joints (R2) and (R3), respectively. Link 6 (*Link B*) is also a rigid link and is connected to link 8 (*V-Link B*) through two revolute joints (R5) and (R6), respectively.

Links 7 (*V-Link A*) and 8 (*V-Link B*) are two V- shape rigid bodies with a V- angle labelled w. These links are connected to rotational link 2 (*Slider A*) by two rotation joints (R1, R4) and are also connected to Rollers A&B by two revolute joints (R9) and (R10). Since the kinematics of the mechanism is being studied regardless of the compliant motion of the *Tool*, we removed the spring from the mechanism.

As mentioned earlier, the mechanism is connected to the curve by two *Rollers A&B*. The mechanism works in such a way that, when the curve moves in the horizontal direction the two

Rollers move over the curve and transfer the motion to links 7 (*V-Link A*) and 8 (*V-Link B*) thereby causing the rotation of these links about the origin of the *Base Link* by the rotation angles $\theta_{a1}$and θ_{b1}, respectively (Fig. 3-7). Next, links 7 & 8 transfer the motion to links 5 (*Link A*) and 6 (*Link B*) through two passive rotations with angles $\theta_{a2}$and θ_{b2} between them respectively. Links 5 (*Link A*) and 6 (*Link B*) then transfer the motion to link 4 (*Tool*) by two other passive rotational joints with angles $\theta_{a3}$and θ_{b3} with respect to the horizontal axis. Links 5 & 6 cause rotation of 4(*Tool*) about the origin of the *Base Link* with an angle α with respect to the vertical axis of the coordinate system.

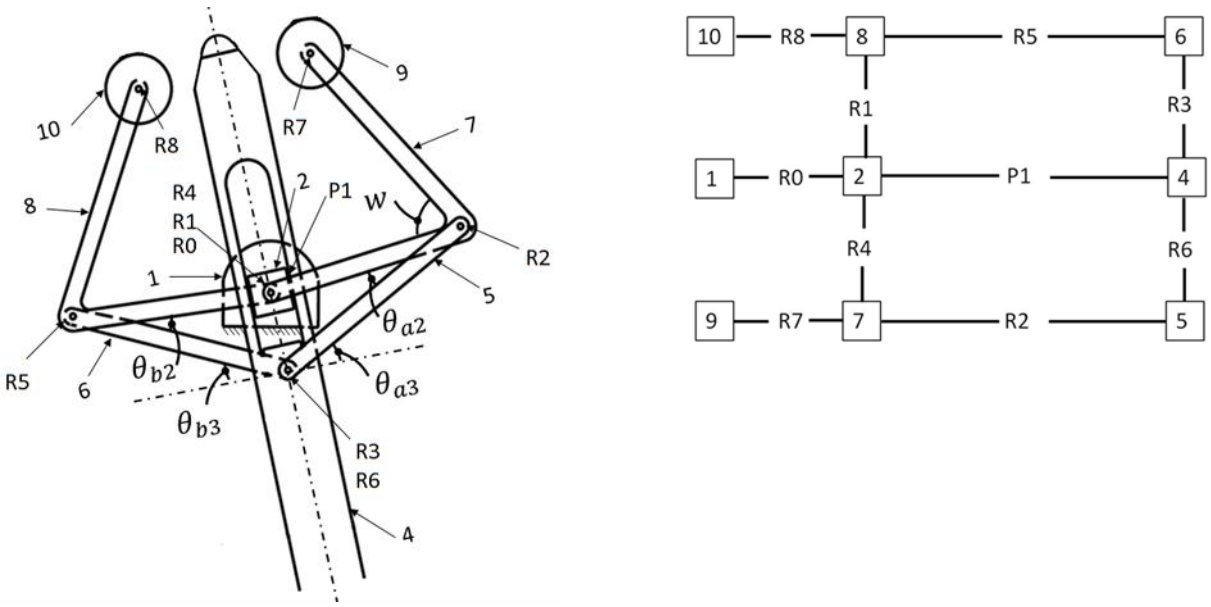

Figure 3-2 : kinematic chain of the mechanism

3.2 Kinematic Problem

A more simplistic kinematic analysis of the mechanism can be done in two steps. First, the mechanism is in a vertical position without connecting to the curve (no machining) and link 2 (*Slider A*) is considered to be the *Base Link*. Link 3 (*Slider B*) is fixed to link 4 (*Tool*). In this case, mechanism has only one-DOF. Second, it is considered to move on a curve (as explained earlier in the kinematic chain) and has two degrees of freedom.

3.2.1 Kinematics for 1-DOF

As shown in Fig. 3-3, in order to identify the maximum working limit of the system, the

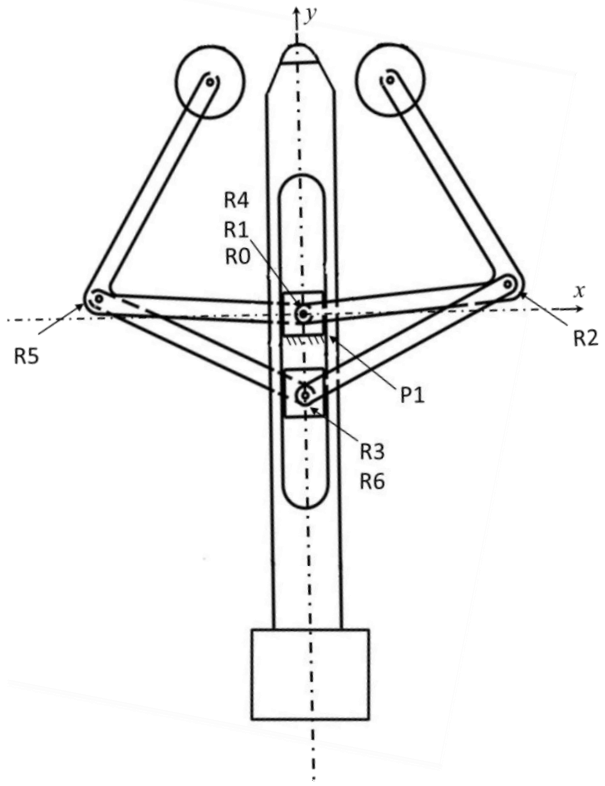

Figure 3-3 : Schematic of the design in 1-DOF

mechanism is assumed to be free of curves. It is also assumed that the rotation of link 2 (*Slider A*) about the origin (R0) is eliminated and link 2 (*Slider A*) is considered to be the *Base Link*. In this case, link 4 (*Tool*) has only one translation movement along the *y*-axis, without rotation, therefore the mechanism has only one degree of freedom.

Links 7 (*V-Link A*) and 8 (*V-Link B*) are connected to the origin of the *Base Link* with two revolute joints (R1, R4). Links 5 (*Link A*) and 6 (*Link B*) are first connected to links 7 (*V-Link A*) and 8 (*V-Link B*) with two passive revolute joints (R2, R5) respectively and then to link 4 (*Tool*) by two other revolute joints (R3, R6).

Figure 3-4 shows the schematic of the design in a coordinate system. Point *O* is the origin of the *Base Link*. If point *C* is the point connecting links 5 (*Link A*) and 6 (*Link B*) with link 4 (*Tool*), it will only have translational movement along the *y*-axis. This means that by moving link 4 (*Tool*)

upward or downward in the *y*-axis direction, links 7 (*V-Link A*) and 8 (*V-Link B*) move symmetrically upward or downward.

a) Degrees of Freedom

The degrees of freedom of a mechanism are the independent parameters or inputs describing a mechanical system. The degrees of freedom of a mechanism can be obtained in terms of the number of links, the number of joints and the types of joints in the mechanism through the following equation [19].

$$F = \lambda(n - j - 1) + \sum_{i=1}^{j} f_i \tag{3.1}$$

F: Degrees of freedom of a mechanism.

f_i: Degrees of relative motion permitted by joint i.

j: Number of joints in a mechanism, assuming that all the joints are binary.

n: Number of links in a mechanism, including the fixed link.

λ: Degrees of freedom of space in which a mechanism is intended to function.

Hence by considering all the links free of constraints, a mechanism consisting of n-links in which one is fixed, the degrees of freedom are $\lambda(n-1)$.

In this case, the following equations define the degrees of freedom.

$$\sum_{i=1}^{7} f_i = 7, \;\; j = 7, \qquad n = 6, \qquad \lambda = 3$$

$$F = 3(6 - 7 - 1) + 7 * 1 = 1$$

b) Position Analysis

In Fig. 3-4, two loops can be identified for each side of the mechanism. l_1, l_2 and l_4, l_5 are the lengths of each side of link 7 (*V-Link A*) and link 8 (*V-Link B*) respectively, l_3 is the length of link 5 (*Link A*), l_6 is the length of link 6 (*Link B*) and r is the distance between point *C* and the origin of the *Base Link*. As it can be seen from the Fig. 3-4, distance r becomes smaller and the two ends of the *V-Links* (7 and 8) come closer to the *y*-axis when moving point *C* toward point *O*.

If $\boldsymbol{r}$ is considered to be the input of the system, the endpoint positions of links 7 (*V-Link A*) and 8 (*V-Link B*) are to be determined as the output of the system via direct kinematics.

The position of the mechanism for the first two loops is as follows:

First loop:

$$x_a = l_1 \cos\theta_{a1} + l_2 \sin\gamma \tag{3.2}$$

$$y_a = l_2 cos\gamma + l_1 sin\theta_{a1} \tag{3.3}$$

Second loop:

$$\theta_{a1} = sin^{-1}\left(\frac{{l_3}^2 - {l_1}^2 - r^2}{2 l_1 r}\right) \tag{3.4}$$

$$\gamma = \frac{\pi}{2} + \theta_{a1} \tag{3.5}$$

By direct kinematics, the coordinates of points A and B will be computed with the given values of r.

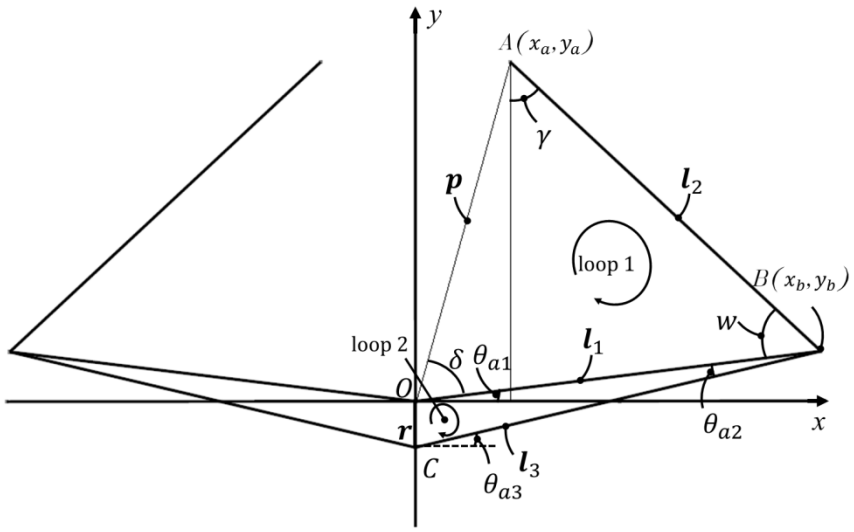

Figure 3-4 : Schematic of the design and its coordinate system

c) Jacobian Matrix for 1-DOF

The matrix by which the joint rates in the actuator space are transformed to the velocity state in the end-effector space is called the Jacobian matrix [6]. In a mechanism, some joints are actuator

joints and others are passive joints. Generally, the number of actuated joints can be considered as degrees of freedom of the mechanism.

If the actuated joint's variables are represented by vector $\boldsymbol{q}$ and the position of the end-effector is represented by a vector $\boldsymbol{x}$, then the kinematic constraint imposed can be written as follows:

$$\mathbf{f}(\boldsymbol{x}, \boldsymbol{q}) = \mathbf{0} \tag{3.6}$$

In this formula, **f** is the function of $\boldsymbol{q}$ and $\boldsymbol{x}$, while **0** is a zero vector.

By differentiating eq. (3.6) with respect to time, the relationship between input joint rate and output joint rate can be obtained.

$$\mathbf{J}_x \dot{\boldsymbol{x}} = \mathbf{J}_q \dot{\boldsymbol{q}}, \tag{3.7}$$

d) Velocity Vector-loop Method

In this method, two different directions of a loop-closure can be used to formulate the velocity vector of a point. Each loop consists of a base, an end point and its links. All the passive joints must be eliminated. To do so, the velocity vector loop equation is dot multiplied with a vector that is normal to all the vectors of the passive joints. The resulting equations are grouped into a Jacobian matrix. Then the end-effector velocity matrix is defined as the six-dimensional vector which consists of linear velocity of the end-effector, that is,

$$\dot{\boldsymbol{x}} = \begin{bmatrix} \mathbf{v}_{\boldsymbol{p}} \\ \boldsymbol{\omega}_{\boldsymbol{p}} \end{bmatrix} \tag{3.8}$$

Let us consider the vector $\boldsymbol{r}$ as the input variable and the position of point *A*, denoted by the vector $\boldsymbol{p}$ with respect to the coordinate system, as the output.

Let the same nomenclature define the vector of each link when it is in bold ($\boldsymbol{l}_1, \boldsymbol{l}_2, \boldsymbol{l}_3, \boldsymbol{r}$).

For this mechanism, the input vector is $\boldsymbol{r} = [0\,, 0\,, r_z]^{\mathrm{T}}$ and the output vector $\boldsymbol{z} = [x\,, y\,, \theta_{a1}]^{\mathrm{T}}$. Since there is only one input and one output, the Jacobian matrix of this mechanism denoted with $\mathbf{J}_z$ is a (1×3) matrix.

From the geometry of the linkage, it is possible to write the loop-closure equation for the first loop:

$$\boldsymbol{l}_1 = \boldsymbol{l}_2 + \boldsymbol{p} \tag{3.9}$$

For the second loop, the vector equation is:

$$\boldsymbol{l}_3 = \boldsymbol{l}_1 + \boldsymbol{r} \tag{3.10}$$

Equations (3.9) and (3.10) give

$$\boldsymbol{p} = \boldsymbol{l}_3 - \boldsymbol{l}_2 - \boldsymbol{r} \tag{3.11}$$

This is a planar mechanism. The angular velocity vectors of all the links point in the positive *z*-direction. By differentiating the two sides of eq.(3.11) with respect to time, a velocity vector loop equation can be derived. Since $\boldsymbol{l_1}$ and $\boldsymbol{l_2}$ are members of the same rigid body, their orientation angles are equal.

$$\dot{\gamma} = \dot{\theta}_{a1} \tag{3.12}$$

$$\dot{\boldsymbol{p}} - (\boldsymbol{k} \times \boldsymbol{l}_3)\dot{\theta}_{a3} - (\boldsymbol{k} \times \boldsymbol{l}_2)\dot{\theta}_{a1} - \dot{\boldsymbol{r}} = \boldsymbol{0},\ \dot{\boldsymbol{r}} = \dot{r}\boldsymbol{e} \tag{3.13}$$

where $\dot{\boldsymbol{p}}$ is the velocity vector of the endpoint of link 7 (point *A*), $\dot{\theta}_1$ is the angular velocity of link 7 (*V-Link A*), $\dot{r}$ is the linear velocity of point *C* and $\boldsymbol{k}$ is the unit vector pointing in the positive *z*-axis direction. In eq.(3.13), $\dot{\theta}_3$ should be eliminated since it is a passive joint variable.

Dot multiplying both sides of eq.(3.13) by vector $\boldsymbol{l}_3$ gives

$$\boldsymbol{l}_3\dot{\boldsymbol{p}} - \boldsymbol{k} \cdot (\boldsymbol{l}_2 \times \boldsymbol{l}_3)\dot{\theta}_{a1} - \boldsymbol{l}_3 \cdot \dot{r}\boldsymbol{e} = \boldsymbol{0} \tag{3.14}$$

By writing (3.14) in matrix form, the relation between input and output velocity can be defined as follows:

$$\mathbf{J}_z\dot{\boldsymbol{z}} = \mathbf{J}_r\dot{\boldsymbol{r}} \tag{3.15}$$

where $\mathbf{J}_z$ is the (1×n) matrix and $\dot{\boldsymbol{r}}$ and $\dot{\boldsymbol{z}}$ are the velocity vectors of the input and output respectively.

$$\dot{\boldsymbol{z}} \equiv \begin{bmatrix} \dot{\boldsymbol{p}} \\ \dot{\theta}_{a1} \end{bmatrix} \equiv \begin{bmatrix} \dot{x} \\ \dot{y} \\ \dot{\theta}_{a1} \end{bmatrix} \tag{3.16}$$

$$\mathbf{J}_z \equiv \begin{bmatrix} l_{3x} & l_{3y} & -\left(l_{2x}l_{3y} - l_{2y}l_{3x}\right) \end{bmatrix} \tag{3.17}$$

$$\mathbf{J}_r \equiv \boldsymbol{l}_3^{\mathrm{T}} \tag{3.18}$$

In order to find $\dot{x}$ and $\dot{y}$ for any given value of $\dot{r}$, the matrix $\mathbf{J}_z$ must be inverted. Given that the dimension of this matrix is (1×3), it is not invertible. But it is possible to do the inverse, which means that $\dot{x}$ and $\dot{y}$ can be found for any given value of the linear velocity $\dot{r}$.

e) Result Validation

For a validation of the Jacobian matrix, the analytical velocity or relative velocity method may be used. In this method, $\dot{\boldsymbol{r}}$ is the velocity vector of point *C* in the *y*-direction and the velocity of point *A* must be evaluated.

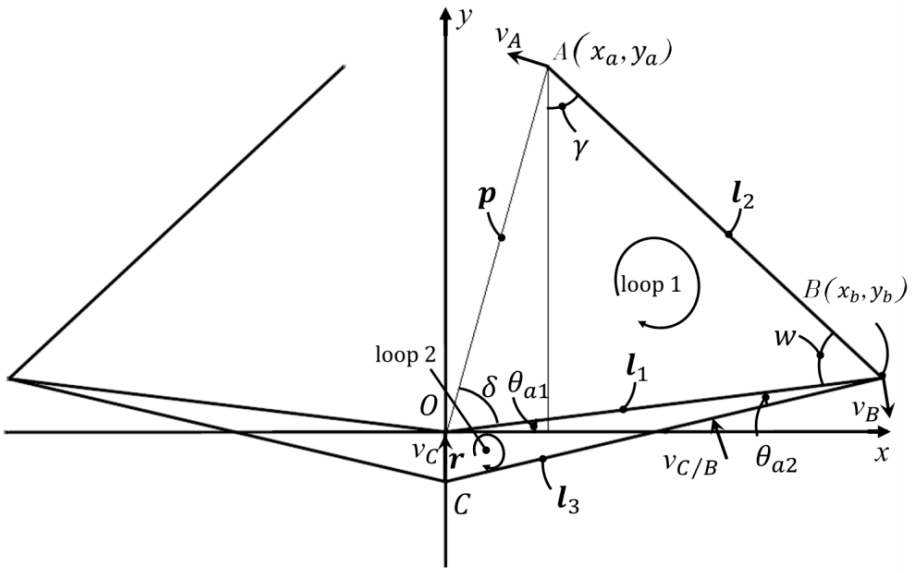

Figure 3-5 : Velocity vectors for right branch of the mechanism

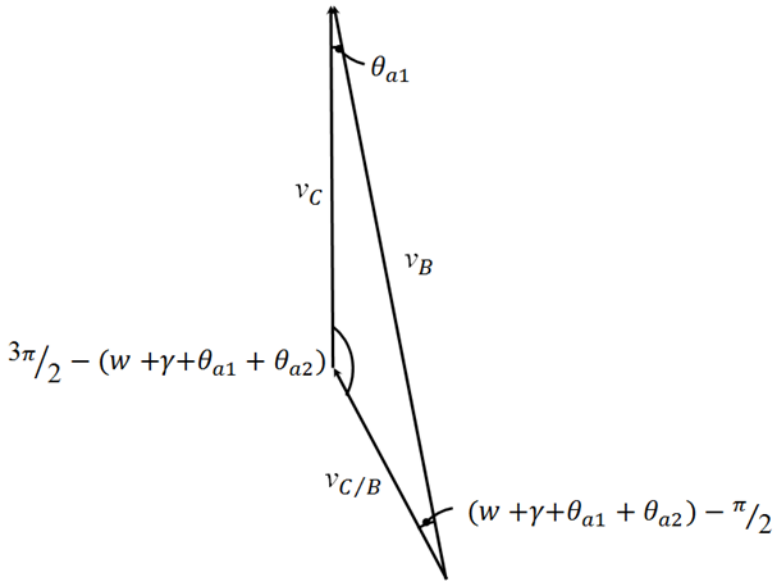

Figure 3-6 : Velocity polygon of the second loop

Figure 3-5 illustrates the velocity vectors for all points. As it can be seen, the velocity of point *B* is normal to vector $\boldsymbol{l}_1$. Since link 5 (*Link A*) is a floating link, the velocity of its points is normal to vector $\boldsymbol{l}_3(v_{(C/B)})$.

By creating the velocity polygon for the second loop, the velocity of point *B* and the velocity of link 7 (*V-Link A*) can be obtained from which the angular velocity of link 7 ($\dot{\theta}_{a1}$) is obtained by eq.(3.20).

In Fig. 3-5, the triangle *AOB* can be considered with dimensions l_1 , l_2 and p (l_1 , l_2 are the lengths of each side of link 7 (*V-Link A)* and link 8 (*V-Link B)* respectively and p is the distance from point *O* to point *A*). Therefore, link 7 (*V-Link A*) and link *OA* will have the same angular velocity obtained by the following equations:

$$\frac{v_C}{\cos(w+\gamma+\theta_{a1})} = \frac{v_B}{\cos(w+\theta_{a1}+\theta_{a2}+\gamma)} \tag{3.19}$$

$$v_B = \frac{v_C \cos(w+\theta_{a1}+\theta_{a2}+\gamma)}{\cos(w+\theta_{a2}+\gamma)} \tag{3.20}$$

From there, the angular velocity $\dot{\theta}_{a1}$ can be obtained from the following equations:

$$v_B = l_1 \dot{\theta}_{a1} \tag{3.21}$$

$$\dot{\theta}_{a1} = \frac{v_B}{l_1} = \dot{\gamma} = \dot{\delta} \tag{3.22}$$

The objective is to find the velocity of point *A*. It can be obtained by using the following equations:

$$v_A = p\dot{\theta}_{a1} \tag{3.23}$$

$$p = \pm\sqrt{{l_1}^2 + {l_2}^2 - 2l_1 l_2 \cos w} \tag{3.24}$$

$$\delta_1 = \sin^{-1}\left(\frac{x}{p}\right) \tag{3.25}$$

By projecting the velocity of point *A* on the x and y axes, $\dot{x}$ and $\dot{y}$ can be found.

$$\dot{x} = v_{Ax} = v_p \sin(\delta + \theta_{a1}) \tag{3.26}$$

$$\dot{y} = v_{Ay} = v_p \cos(\delta + \theta_{a1}) \tag{3.27}$$

By programming in Matlab, it is possible to compute the $\dot{x}$ and $\dot{y}$ for any given value of $\dot{r}$. For instance, for $\dot{r}_y$ =1mm/s:

$\dot{x}$= 0.8010 mm/s

$\dot{y}$ = 0.3324 mm/s

$\dot{\theta}_{a1}$= 0.0201 rad/s

By now putting these values in the matrix $\dot{\boldsymbol{z}}$ in eq.(3.15), the obtained value for $\dot{r}_{\mathrm{y}}$ must be 1.

3.2.2 Kinematics of 2-DOF

Figure 3-7 shows the schematic of the design and its coordinate system for two degrees of freedom. In this case the mechanism moves on the curve and has two degrees of freedom. It means that each side of the system can move independently and cause the rotation of link 4 (*Tool*) about the origin of the coordinate system.

a) Degrees of Freedom

In this case, from Fig. 3-1, we have:

$$\sum_{i=1}^{8} f_i = 8, \;\; j = 8, \qquad n = 7, \qquad \lambda = 3$$

Substituting these data in eq.(3.1) gives:

$$F = 3(7 - 8 - 1) + 8 * 1 = 2$$

b) Position Analysis

Here α is the orientation angle of link 4 (*Tool*) about the center and x_{a}, y_{a} and x_{b}, y_{b} are the

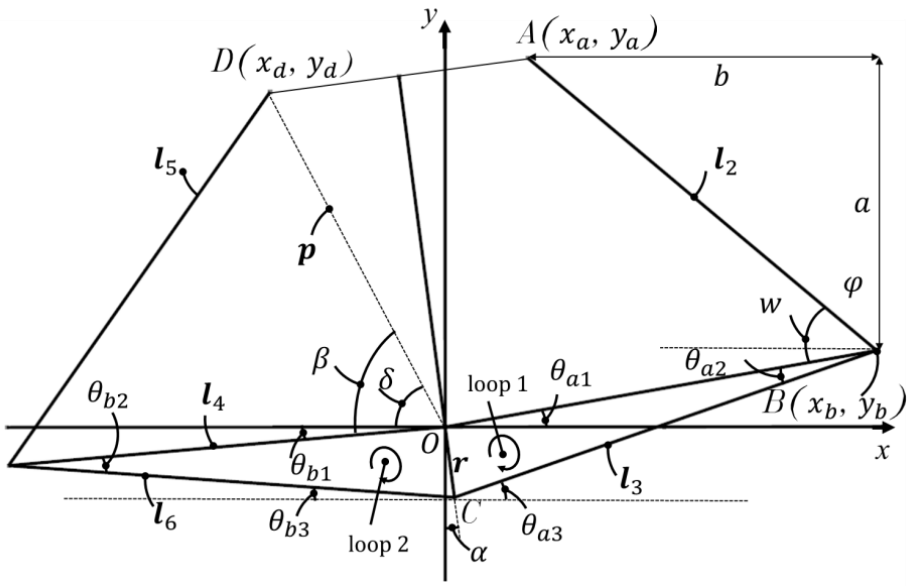

Figure 3-7 : Schematic of the design and its coordinate system for two degrees of freedom

positions of endpoint links 7 (*V-Link A*) and 8 (*V-Link B*) respectively and α can be found for any coordinates of the endpoints.

$$\delta = \beta - \theta_{a1},\ \varphi = w - \theta_{a1} \tag{3.28}$$

$$\begin{cases} x_d = p\cos\delta \\ y_d = p\sin\delta \\ a = l_2\sin\varphi \\ b = l_2\cos\varphi \\ y_b = l_1\cos\theta_{a1} \\ x_b = l_1\sin\theta_{a1} \\ y_a = a + y_b \\ x_a = x_b - b \end{cases} \tag{3.29}$$

$$\alpha = \tan^{-1}\left(\frac{y_a - y_d}{x_a - x_d}\right) \tag{3.30}$$

$$r = \pm\sqrt{{l_1}^2 + {l_3}^2 - 2l_1 l_3\cos\theta_{a2}} \tag{3.31}$$

$$p = \pm\sqrt{{l_1}^2 + {l_2}^2 - 2l_1 l_2\cos w} \tag{3.32}$$

c) Jacobian Matrix

In this case, the input vector is $\boldsymbol{q} \equiv [\theta_{a1} \quad \theta_{b1}]^{\mathrm{T}}$ and the output vector is $\boldsymbol{z} \equiv [r_x \quad r_y \quad \alpha]^{\mathrm{T}}$. A loop-closure equation can be written for loop 1 as follows:

$$\boldsymbol{l}_3 = \boldsymbol{l}_1 + \boldsymbol{r} \tag{3.33}$$

By taking the derivative of eq.(3.33) with respect to time, we obtain

$$(\boldsymbol{k} \times \boldsymbol{l}_3)\dot{\theta}_{a3} = (\boldsymbol{k} \times \boldsymbol{l}_1)\dot{\theta}_{a1} + \dot{\boldsymbol{r}} + \boldsymbol{r}\dot{\alpha},\ \dot{\boldsymbol{r}} = \dot{r}\boldsymbol{e} \tag{3.34}$$

where $\boldsymbol{k}$ is the unit vector pointing in the positive k direction and $\dot{\boldsymbol{r}}$ is the velocity vector of point C. Since $\dot{\theta}_3$ is a passive joint variable and must be eliminated, dot-multipling both sides of eq.(3.34) by the vector $\boldsymbol{l}_3$ gives :

$$\boldsymbol{l}_3 \cdot \dot{\boldsymbol{r}} + \boldsymbol{k} \cdot (\boldsymbol{r} \times \boldsymbol{l}_3)\dot{\alpha} = -\boldsymbol{k} \cdot (\boldsymbol{l}_1 \times \boldsymbol{l}_3)\dot{\theta}_{a1} \tag{3.35}$$

Writing the same equations for the second loop:

$$\boldsymbol{l}_6 = \boldsymbol{l}_4 + \boldsymbol{r} \tag{3.36}$$

$$\dot{r}\boldsymbol{e} + \boldsymbol{r}\dot{\alpha} = (\boldsymbol{k} \times \boldsymbol{l}_6)\dot{\theta}_{b3} - (\boldsymbol{k} \times \boldsymbol{l}_4)\dot{\theta}_{b1} \tag{3.37}$$

$$\boldsymbol{l}_6 \cdot \dot{\boldsymbol{r}} + \boldsymbol{k} \cdot (\boldsymbol{r} \times \boldsymbol{l}_6)\dot{\alpha} = -\boldsymbol{k} \cdot (\boldsymbol{l}_4 \times \boldsymbol{l}_6)\dot{\theta}_{b1} \tag{3.38}$$

The equations (3.35) and (3.38) can be arranged in the matrix form as follows:

$$\mathbf{J}_z \dot{\boldsymbol{z}} = \mathbf{J}_q \dot{\boldsymbol{q}} \tag{3.39}$$

In this equation $\dot{\boldsymbol{z}}$ is the cartesian velocity and $\dot{\boldsymbol{q}}$ is the joint velocity. In order to find $\dot{\boldsymbol{z}}$, the matrix $\mathbf{J}_z$ must be inverted, yet this matrix is (2×3) and is therefore not invertible.

To invert this matrix, the following formula is used:

$$\mathbf{J}_z{}^{-1} = \mathbf{J}_z{}^{T}\left(\mathbf{J}_z\mathbf{J}_z{}^{\mathrm{T}}\right)^{-1} \tag{3.40}$$

$$\mathbf{J}_z \equiv \begin{bmatrix} \boldsymbol{l}_3{}^{\mathrm{T}} & (\boldsymbol{r} \times \boldsymbol{l}_3)^{\mathbf{T}} \\ \boldsymbol{l}_6{}^{\mathrm{T}} & (\boldsymbol{r} \times \boldsymbol{l}_6)^{\mathbf{T}} \end{bmatrix} \tag{3.41}$$

$$\dot{\boldsymbol{z}} \equiv \begin{bmatrix} \dot{r}_x \\ \dot{r}_y \\ \dot{\alpha} \end{bmatrix} \tag{3.42}$$

$$\mathbf{J}_z = \begin{bmatrix} l_{3x} & l_{3y} & r_x l_{3y} - r_y l_{3x} \\ l_{6x} & l_{6y} & r_x l_{6y} - r_y l_{6x} \end{bmatrix} \tag{3.43}$$

$$\mathbf{J}_q = \begin{bmatrix} -(\boldsymbol{l}_1 \times \boldsymbol{l}_3) \\ -(\boldsymbol{l}_1 \times \boldsymbol{l}_3) \end{bmatrix} \tag{3.44}$$

$$\mathbf{J}_q = \begin{bmatrix} -\left(l_{1x} l_{3y} - l_{1y} l_{3x}\right) \\ -\left(l_{4x} l_{6y} - l_{4y} l_{6x}\right) \end{bmatrix} \tag{3.45}$$

$$\dot{\boldsymbol{q}} \equiv \begin{bmatrix} \dot{\theta}_{a1} \\ \dot{\theta}_{b1} \end{bmatrix} \tag{3.46}$$

d) Result Validation

For validation of the results, the position vector loop equations are used. In this method, the variables associated with degrees of freedom of the mechanism are called primary variables and the remaining variables are known as secondary variables [20].

$$f_1(q, s_1, s_2, \dots s_{N2}) = 0 \tag{3.47}$$

$$f_2(q, s_1, s_2, \dots s_{N2}) = 0 \tag{3.48}$$

where q = generalized coordinate, and
s_i =secondary coordinates, $i = 1, 2, \dots N_2$.
The system of equation for each loop of mechanism is as follows:

$$\begin{cases} l_1\cos\theta_{a1} + r\cos\alpha = l_{a3}\cos\theta_{a3} \\ r\cos\alpha + l_3\sin\theta_{a3} = l_1\cos\theta_{a1} \\ r\sin\alpha + l_6\cos\theta_{b3} = l_4\cos\theta_{b1} \\ r\cos\alpha + l_4\cos\theta_{b1} = l_6\cos\theta_{b3} \end{cases} \tag{3.49}$$

By differentiating the position loop functions (f_i) with respect to the secondary coordinates, the Jacobian matrix can be formed:

$$\left[\frac{\partial f}{\partial s}\right] = \begin{bmatrix} \frac{\partial f_1}{\partial s_1} & \frac{\partial f_1}{\partial s_2} & \frac{\partial f_1}{\partial s_3} \dots\dots & \frac{\partial f_1}{\partial s_{N1}} \\ \frac{\partial f_2}{\partial s_1} & \frac{\partial f_2}{\partial s_1} & \frac{\partial f_2}{\partial s_1} \dots\dots & \frac{\partial f_2}{\partial s_{N1}} \\ \vdots & \vdots & \vdots & \vdots \\ \frac{\partial f_{N2}}{\partial s_1} & \frac{\partial f_{N2}}{\partial s_2} & \frac{\partial f_{N2}}{\partial s_3} \dots\dots & \frac{\partial f_{N2}}{\partial s_{N2}} \end{bmatrix} \tag{3.50}$$

$$\begin{cases} \dot{r}\sin\alpha + r\cos\alpha\dot{\alpha} + l_3\sin\theta_{a3}\dot{\theta}_{a3} = l_1\sin\theta_{a1}\dot{\theta}_{a1} \\ \dot{r}\cos\alpha + r\sin\alpha\dot{\alpha} + l_3\cos\theta_{a3}\dot{\theta}_{a3} = l_1\cos\theta_{a1}\dot{\theta}_{a1} \\ \dot{r}\sin\alpha + r\cos\alpha\dot{\alpha} + l_6\sin\theta_{b3}\dot{\theta}_{b3} = l_4\sin\theta_{b1}\dot{\theta}_{b1} \\ \dot{r}\cos\alpha + r\sin\alpha\dot{\alpha} + l_6\cos\theta_{b3}\dot{\theta}_{b3} = l_4\cos\theta_{b1}\dot{\theta}_{b1} \end{cases} \tag{3.51}$$

$$\mathbf{J}_q\dot{\boldsymbol{q}} = \mathbf{J}_z\dot{\boldsymbol{z}} \tag{3.52}$$

$$\mathbf{J}_q = \begin{bmatrix} \sin\alpha & r\sin\alpha & l_3\sin\theta_{a3} & 0 \\ \cos\alpha & -r\sin\alpha & l_3\cos\theta_{a3} & 0 \\ \sin\alpha & r\cos\alpha & 0 & -l_6\sin\theta_{b3} \\ \cos\alpha & -r\sin\alpha & 0 & -l_6\cos\theta_{b3} \end{bmatrix} \tag{3.53}$$

$$\dot{\boldsymbol{z}} \equiv \begin{bmatrix} \dot{r} \\ \dot{\alpha} \\ \dot{\theta}_{a3} \\ \dot{\theta}_{b3} \end{bmatrix} \tag{3.54}$$

$$\mathbf{J}_q = \begin{bmatrix} l_1 \sin\theta_{a1} & 0 \\ l_1 cos\theta_{a1} & 0 \\ 0 & -l_4 cos\theta_{b1} \\ 0 & -l_4 cos\theta_{b1} \end{bmatrix} \tag{3.55}$$

$$\dot{\boldsymbol{q}} \equiv \begin{bmatrix} \dot{\theta}_{a1} \\ \dot{\theta}_{b1} \end{bmatrix} \tag{3.56}$$

3.3 Conclusion

In this chapter, a passive 2-DOF planar mechanism is presented for machining the wavy surface by using two contact points. The closed form kinematic equations for this mechanism have been developed based on the obtained relationship for the orientation angle of the verified *Tool*.

In the next chapter, we will use this concept in order to develop a passive spatial 3-DOF mechanism for machining of curved panels.

CHAPITRE 4 DESIGN OF A PASSIVE MECHANISM FOR MACHINING PURPOSE

In the introduction, some mechanical methods for this purpose were introduced. The last method was mirror milling created by the airbus company. As mentioned, this method uses two machines working together based on the mirror system. Despite the advantages of this method, fabrication cost is high.

In this chapter, we are looking for a mechanical system which is less costly yet competent. Therefore, our objective is to design a mechanism which can be mounted on a robot wrist, provide the orientation of the cutting tool without the need of precise information about the geometry of the cutting surface as well as maintain contact between tool and surface by using three sliding pads.

This chapter describes the design of a passively 3-DOF spatial parallel mechanism which can be used for the machining of curved panels without prior knowledge of their precise geometry. This mechanism is a somewhat zero-torsion manipulator with three degrees of freedom (one translation along the *z*-axis and two orientations). This mechanism is designed such that the translational degree of freedom is passive and is controlled by the robot motion.

4.1 Kinematic Chain

Figure 4-1 shows the Overview of this mechanism which is connected to a robot wrist and placed over the curved panels by using three contact points. Apparently, the mechanism moves over the panel where the cutting tool is aligned normal to the surface and continually in contact with the surface.

The mechanism is composed of three major systems, where each of these systems is designed to perform a special task. These three systems are as follows:

- A 3-PSP system in order to provide the orientation of the cutting tool.
- A system in order to keep the contact between the cutting tool and the surface.
- A system to adjust the depth of cut before starting the cutting operation.

This mechanism is composed of 18 links. Table 4-1 and 4-2 show the number and name of the links used in this mechanism.

a) 3-PSP System

In this system three chains for the orientation of the cutting tool can be identified. Each chain is composed of two passive prismatic joints and one passive spherical joint. Link 1 is considered to be the *Base Link*. Three cylinders are fixed vertically to the *Base Link* at 120 ° angle relative to each other. Within the cylinders, three springs are located to provide the compliant motion of the mechanism during machining.

Links 6, 7 and 8 (*Slider A*, *Slider B*, *Slider C*) are connected to the *Base Link* (place inside the cylinders) through three passive prismatic joints (P2, P3, and P4). These three links at the end of which three spherical joints move are parallel. Link 2 is considered to be the *Tool holder* and the tool is placed inside it.

As shown in Fig. 4-1, three other links 9, 10 and 11 (*Slider D*, *Slider E*, *Slider F*) are fixed to the *Tool holder* and are connected to links 6, 7 and 8 (*Slider A*, *Slider B*, *Slider C*) through three passive spherical joints (S1, S2, and S3). As the mechanism moves and changes its position over the surface, links 6, 7 and 8 (*Slider A*, *Slider B*, *Slider C*) transfer the movement to the three passive spherical joints (S1, S2, and S3) and then these spherical joints slide inside links 9, 10 and 11 (*Slider D*, *Slider E*, *Slider F*) through three passive prismatic joints (P5, P6, and P7) and cause the orientation of the *Tool holder*.

b) Connection System:

From Fig. 4-1 links 3, 4, and 5 (*L-Link A, L-Link B, L-Link C*) can be identified. These 3 links are attached to the tool holder by using 3 revolute joints (R1, R2, R3) and are also in contact with the surface via three *Balls* 12, 13 and 14 (*Ball A, Ball B, Ball C*) used as three sliding pads. As the mechanism moves over the surface with the aid of these three *Balls*, this system maintains contact between the tool and surface during machining.

c) Adjusting System:

In order to adjust the depth of cut before cutting, we use a system with three chains consisting of 4 links, 6 revolutes and one prismatic joint.

Three links 15, 16 and 17 (*Link A, Link B, Link C*) are connected to links 3, 4, and 5 (*L-Link A, L-Link B, L-Link C*) with three revolute joints (R7, R8, R9) and again are connected to link 18 (*Adjusting disc*) via three revolute joints (R4, R5, R6). Then the link 18 (*Adjusting disc*) is connected to the *Tool holder* with a prismatic joint (P1).

In order to adjust the depth of cut (distance between cutting tool and surface) the link 18 (*adjusting disc*) can be move up and down along the axes of the tool by using the prismatic joint (P1).

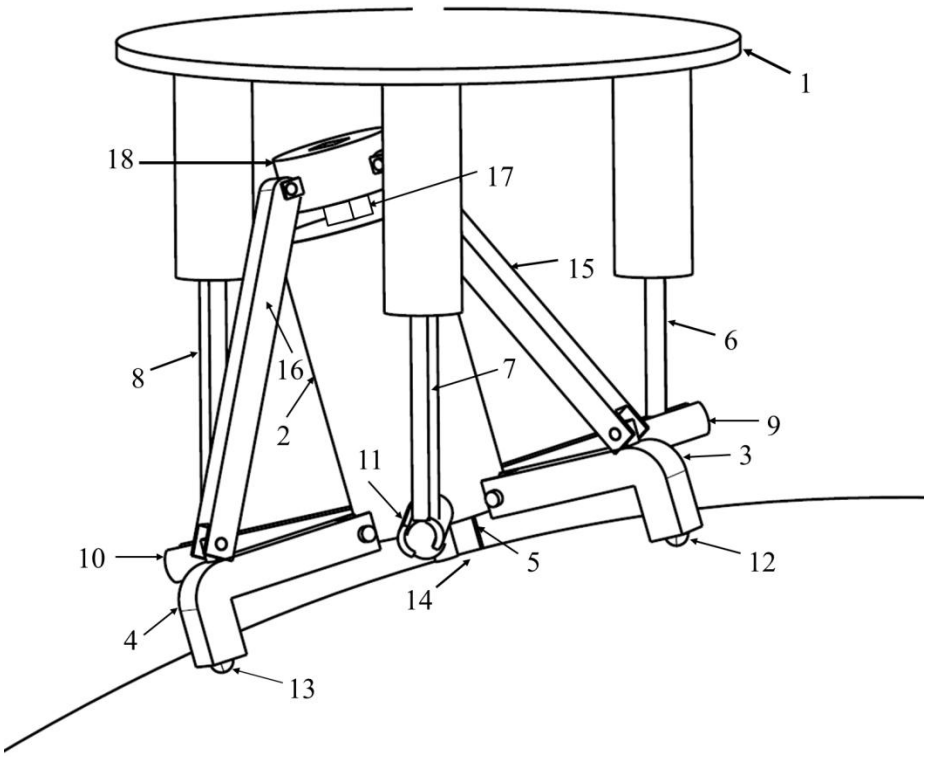

Figure 4-1 : Overview of the mechanism.

Link 17(*Link C*) is behind of link 18 (*Adjusting disc*) and link 14(*Ball C*) is behind of surface.

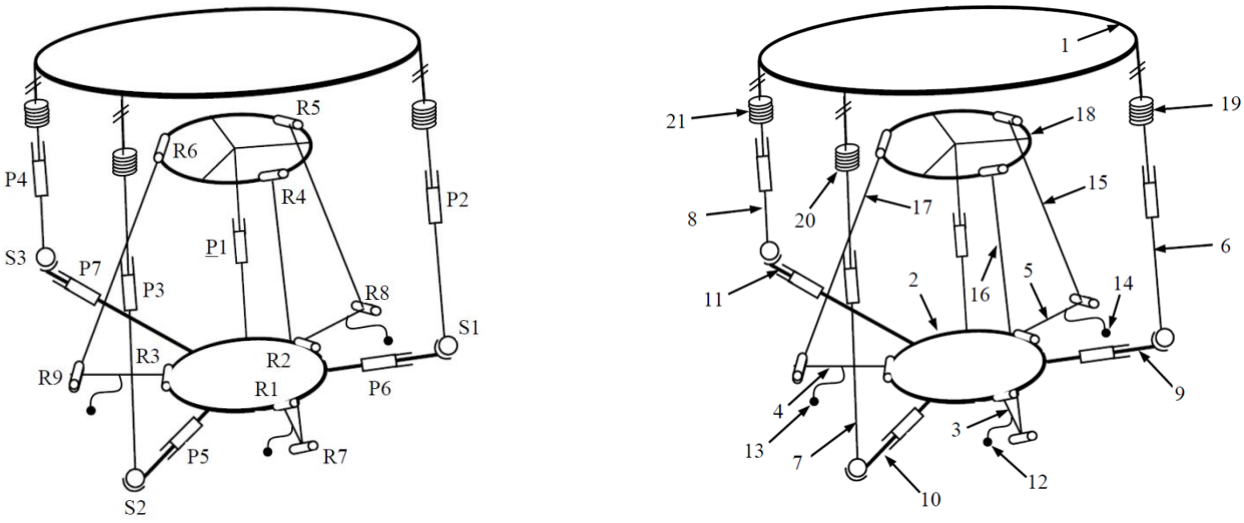

(a) (b)

Figure 4-2 : Kinematic chain of the mechanism, (a) Joint numbers, (b) Link Numbers

Table 4-1: Link identification

No.	Link name	No.	Link name
1	*Base Link*	12	*Ball A*
2	*Tool holder*	13	*Ball B*
3	*L-Link A*	14	*Ball C*
4	*L-Link B*	15	*Link A*
5	*L-Link C*	16	*Link B*
6	*Slider A*	17	*Link C*
7	*Slider B*	18	*Adjusting Disc*
8	*Slider C*	19	*Spring A*
9	*Slider D*	20	*Spring B*
10	*Slider E*	21	*Spring C*
11	*Slider F*		

Table 4-2 : Joint identification

Joint	Link connection
R1	Revolute joint between links 2 & 3
R2	Revolute joint between links 2 & 4
R3	Revolute joint between links 2 & 5
R4	Revolute joint between links 18 &16
R5	Revolute joint between links 18 &15
R6	Revolute joint between links 18 &17
R7	Revolute joint between links 3 & 16
R8	Revolute joint between links 5 & 15
R9	Revolute joint between links 4 & 17
P1	Prismatic joint between links 18 & 2

Joint	Link connection
P2	Prismatic joint between links 1 & 6
P3	Prismatic joint between links 1 & 7
P4	Prismatic joint between links 1 & 8
P5	Prismatic joint between links 7 & 10
P6	Prismatic joint between links 6 & 9
P7	Prismatic joint between links 8 & 11
S1	Spherical joint between links 6 & 9
S2	Spherical joint between links 7 & 10
S3	Spherical joint between links 8 & 11

4.2 Inverse kinematics

In order to solve this problem, let us attach frame *B* to the moving platform, named here B, and frame *A* to the base link named here A. We arbitrarily chose to locate this origin to the center point of the base frame. The first Cartesian coordinate system denoted as $O\ (x, y, z)$ is attached to the base platform and the second Cartesian coordinate system denoted as $\acute{O}\ (u, v, w)$ is attached to the moving platform center.

In inverse kinematics, the idea is to find the position of the vertical prismatic joints when the pose of the moving platform is known. For this mechanism, the orientation of the moving platform described by the tilt-and-torsion angle and its z-coordinate are given, yet the prismatic values must be found. Figure 4-3 shows the kinematic model of the 3-PSP system. Let the position vector at the center of the moving platform with respect to the frame A be $\boldsymbol{p}$.

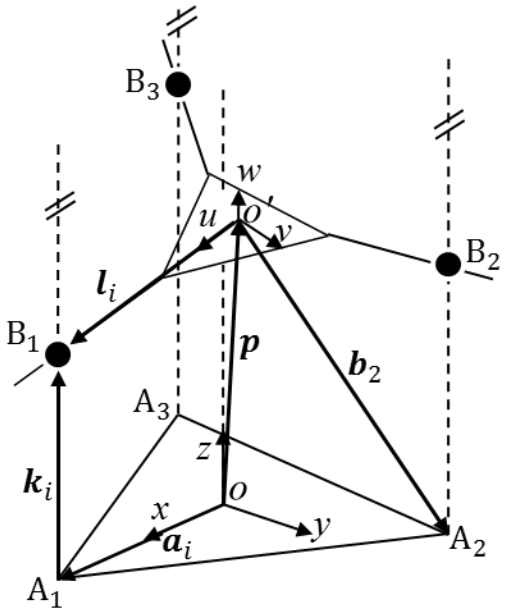

Figure 4-3 : Kinematic model of the 3-PSP mechanism

$$\boldsymbol{p} = [x \quad y \quad z]^{\mathrm{T}},\ \boldsymbol{a}_i = d[\cos\alpha_i \sin\alpha_i \ \ 0]^{\mathrm{T}},\ \boldsymbol{k_i} = [0 \ \ 0 \ \ q_i], \tag{4.1}$$

Since the base and the moving platform are symmetric, let $\boldsymbol{m}_i$ is the unit vector at the center of frame *B* and is directed along the vector $\boldsymbol{l}_i$**,** then it can be written as:

$$^{B}\boldsymbol{m}_i = [\cos\alpha_i \ \sin\alpha_i \ \ 0]^{\mathrm{T}} \tag{4.2}$$

where α_i is the angle between the three kinematic chains and defined by α_i=2(i-1)$\pi/3$ (i= 1,2,3). In order to express the three unit vectors of frame B in the base frame A, the following equation can be used:

$$^{A}\boldsymbol{m}_i = \boldsymbol{Q}\ ^{B}\boldsymbol{m}_{i.} \tag{4.3}$$

where $\boldsymbol{Q}$ is the rotation matrix described by the tilt-and-torsion angle, as mentioned in the previous chapter.

$$\boldsymbol{Q}(\emptyset,\theta) = \begin{bmatrix} \cos^2\emptyset\cos\theta + \sin^2\emptyset & \sin\emptyset\cos\emptyset(\cos\theta - 1) & \cos\emptyset\sin\theta \\ \sin\emptyset\cos\emptyset(\cos\theta - 1) & \sin^2\emptyset\cos\theta + \cos^2\emptyset & \sin\emptyset\sin\theta \\ -\sin\theta\cos\emptyset & -\sin\theta\sin\emptyset & \cos\theta \end{bmatrix} \tag{4.4}$$

The vector $\boldsymbol{a_i}$, originating from the center of the base frame with unit vector $\boldsymbol{v}_i$, is the position vector of point A_i.

$$\boldsymbol{a}_i = d[\cos\alpha_i \sin\alpha_i\ \ 0]^{T} \tag{4.5}$$

where d is the radius of the circle passing points A_1, A_2, A_3.

The vector $\boldsymbol{b}_i$ chosen from the center of platform B to point A_i, can be written as

$$\boldsymbol{b}_i = \boldsymbol{p} - \boldsymbol{a}_i \tag{4.6}$$

The $\boldsymbol{b}_i$, $\boldsymbol{m}_i$ and $\boldsymbol{k_i}$ are coplanar and the following kinematic equations can be written according to the geometrical relationships of parallel mechanisms [23].

$$\det[\boldsymbol{b}_i \quad \boldsymbol{m}_i \quad \boldsymbol{k}] = 0 \tag{4.7}$$

$$l_i\boldsymbol{m}_i + \boldsymbol{b}_i = q_i\boldsymbol{k} = \boldsymbol{k_i} \tag{4.8}$$

where $\boldsymbol{k}$ is the unit vector along the z-axis in frame A and l_i is the distance from the center of the moving platform to the passive spherical joints and q_i is the length directed from A_i to B_i

The feasible motion of the platform can be written as:

$$\begin{cases} x = d\frac{\cos\theta - 1}{4\cos\theta}[\cos4\emptyset(\cos\theta - 1) + \cos2\emptyset(\cos\theta + 1)], \\ y = d\frac{\cos\theta - 1}{4\cos\theta}[sin4\emptyset(\cos\theta - 1) - \sin2\emptyset(\cos\theta + 1)], \end{cases} \tag{4.9}$$

In order to find the passive prismatic joint values q_i , loop closure equations can be used. For each kinematic chain, a loop can be identified as follows:

$$\boldsymbol{p} - l_i\boldsymbol{m}_i - \boldsymbol{r_i} = \boldsymbol{0} \tag{4.10}$$

The vector from point O to point B_i in coordinate frame A can be written as

$$\boldsymbol{r_i} = \boldsymbol{k_i} + \boldsymbol{a}_i \tag{4.11}$$

Substituting the eq.(4.3) and (4.11) with eq.(4.10), we obtain:

$$\boldsymbol{p} - \boldsymbol{l}_i \boldsymbol{Q}(\emptyset, \theta)\, {}^{B}\boldsymbol{m}_i - \boldsymbol{k_i} - \boldsymbol{a}_i = \boldsymbol{0},\ i = 1, 2, 3 \tag{4.12}$$

where $$\boldsymbol{k_1} = [0\ \ 0\ \ q_1], \boldsymbol{k_2} = [0\ \ 0\ \ q_2], \boldsymbol{k_3} = [0\ \ 0\ \ q_3] \tag{4.13}$$

and $$\boldsymbol{m}_1 = \begin{bmatrix} Q_{11} \\ Q_{21} \\ Q_{31} \end{bmatrix}, \boldsymbol{m}_2 = 1/2 \begin{bmatrix} -Q_{11} + \sqrt{3}Q_{12} \\ -Q_{21} + \sqrt{3}Q_{22} \\ -Q_{31} + \sqrt{3}Q_{32} \end{bmatrix}, \boldsymbol{m}_3 = 1/2 \begin{bmatrix} -Q_{11} - \sqrt{3}Q_{12} \\ -Q_{21} - \sqrt{3}Q_{22} \\ -Q_{31} - \sqrt{3}Q_{32} \end{bmatrix} \tag{4.14}$$

where Q_{ij} is the element of *i*th row and *j*th column in the matrix $\boldsymbol{Q}$.

By expanding the derived equations in eq.(4.12) the following equations can be obtained:

$$\begin{cases} x - \boldsymbol{l}_1 Q_{11} - d = 0 \\ y - \boldsymbol{l}_1 Q_{21} = 0 \\ z - \boldsymbol{l}_1 Q_{31} - q_1 = 0 \end{cases} \tag{4.15}$$

$$\begin{cases} x + \boldsymbol{l}_2/2(Q_{11} - \sqrt{3}Q_{12}) + d/2 = 0 \\ y + \boldsymbol{l}_2/2(Q_{21} - \sqrt{3}Q_{22}) + \sqrt{3}d/2 = 0 \\ z + \boldsymbol{l}_2/2(Q_{31} - \sqrt{3}Q_{32}) - q_1 = 0 \end{cases} \tag{4.16}$$

$$\begin{cases} x + \boldsymbol{l}_3/2(Q_{11} + \sqrt{3}Q_{12}) + d/2 = 0 \\ y + \boldsymbol{l}_3/2(Q_{21} + \sqrt{3}Q_{22}) - \sqrt{3}d/2 = 0 \\ z + \boldsymbol{l}_3/2(Q_{31} + \sqrt{3}Q_{32}) - q_3 = 0 \end{cases} \tag{4.17}$$

Finally, the invers kinematic model is given as:

$$\begin{aligned} q_1 &= -\frac{x-d}{Q_{11}} Q_{31} + z \\ q_2 &= -\frac{x-d}{Q_{11} - \sqrt{3}Q_{12}} \left(-Q_{31} + \sqrt{3}Q_{32}\right) + z \\ q_3 &= \frac{x + \frac{d}{2}}{Q_{11} - \sqrt{3}Q_{12}} (-Q_{31} - \sqrt{3}Q_{32}) + z \end{aligned} \tag{4.18}$$

Where the prismatic joint position q_i can be computed from $\boldsymbol{Q}$ and z, while $\boldsymbol{Q}$ depends only on two independent variable as in eq.(4.4).

4.3 Wrenches and Reciprocal Screws

In order to describe either finite or infinitesimal displacement of a rigid body in three-dimensional space, the twist method can be used. All the forces and couples acting on a rigid body can be reduced to a point. The combination of the resultant force **f** and the couple **c** acts along and about a unique axis called a wrench axis or a screw axis. The ratio of the couple to the force is defined as the pitch of the wrench [6].

The unit wrench $\hat{\$}_r$ is described by a pair of vectors. For pure force and for pure couple, the unit wrench is:

$$\hat{\$}_r = \begin{bmatrix} \mathbf{s}_r \\ \mathbf{s}_{ro} \times \mathbf{s}_r \end{bmatrix}, \hat{\$}_r = \begin{bmatrix} 0 \\ \mathbf{s}_r \end{bmatrix} \tag{4.19}$$

where $\mathbf{s}_r$ is a unit vector along the screw axis, $\mathbf{s}_{ro}$ is the vector pointing from the reference frame to the any point on the axis of the screw and $\mathbf{s}_{ro} \times \mathbf{s}_r$ is the moment of the axis of the screw about the reference frame origin.

4.3.1 Reciprocal Screws

Two screws are defined as reciprocal screws when a wrench acting on a rigid body makes the body undergo an infinitesimal twist without producing work. Reciprocal screws of several kinematic pairs are as follows:

- Revolute joint: The unit screw of a revolute joint is along the axis of a joint with zero pitch. In this case, the zero-pitch reciprocal screws are placed on the plane of the revolute joint axis and form a 5-system.
- Prismatic joint: The unit screw of a prismatic joint is along the sliding direction with an infinite pitch and the zero-pitch reciprocal screws lie on the planes perpendicular to the sliding axis.
- Spherical joint: The unit screws pass through the center of the joint and are zero pitch. The zero-pitch reciprocal screws pass through the center of the sphere and form a 3-system.
- Universal joint: The unit screws pass through the center of the universal joint and form a zero-pitch 2-system. In this type of joint, the reciprocal screws pass through the center of the universal joint and are placed on the plane containing the axis of the universal joint.

The readers who are interested in a more detailed description of the screw theory are referred to [7].

4.3.2 Screw-Based Jacobian

Our parallel mechanism comprised of several legs and each contains several links connected by kinematic pairs. Some of these kinematic pairs are actuated, while others are passive. Each leg can be considered as an open-loop chain and a combination of l instantaneous twists ($\$_p$). A linear combination of these instantaneous twists can express the moving platform.

$$\$_p = \sum_{i=1}^{l} \dot{q}_{j,i}\, \hat{\$}_{j,i} \text{ for } i = 1, 2, 3, ..., m, \qquad (m, \text{ is the number of the limbs}) \tag{4.20}$$

Where $\dot{q}_{j,i}$ is the intensity and the $\hat{\$}_{j,i}$ is the unit screw of the jth joint of the ith leg and m is the number of limbs. The end-effector twist can be defined as:

$$\$_p = \begin{bmatrix} \boldsymbol{\omega}_n \\ \mathbf{v}_0 \end{bmatrix} \tag{4.21}$$

Where $\boldsymbol{\omega}_n$ is the angular velocity and $\mathbf{v}_0$ is the linear velocity of the end-effector.

All the passive joint screws can be eliminated by using the theory of reciprocal screws. Taking the orthogonal product of both sides of eq.(4.20) with each reciprocal screw gives g equations which is equal to the number of joints in each leg.

$$\mathbf{J}_{i,x}\$_p = \mathbf{J}_{i,q}\dot{\boldsymbol{q}}_i \tag{4.22}$$

$$\mathbf{J}_{x,i} = \begin{bmatrix} \hat{\$}_{ri,1}^{\mathrm{T}} \\ \hat{\$}_{ri,2}^{\mathrm{T}} \\ \vdots \\ \hat{\$}_{ri,\mathrm{g}}^{\mathrm{T}} \end{bmatrix}, \tag{4.23}$$

$$\mathbf{J}_{q,i} = \begin{bmatrix} \hat{\$}_{r1,1}^{\mathrm{T}}\hat{\$}_{1,1} & 0 & \cdots & 0 \\ 0 & \hat{\$}_{r1,2}^{\mathrm{T}}\hat{\$}_{1,2} & \cdots & 0 \\ \vdots & \vdots & \cdots & \vdots \\ 0 & 0 & \cdots & \hat{\$}_{r1,\mathrm{g}}^{\mathrm{T}}\hat{\$}_{1,\mathrm{g}} \end{bmatrix} \tag{4.24}$$

$$\dot{\boldsymbol{q}} = [\dot{q}_{1,1} \quad \cdots \quad \dot{q}_{1,\mathrm{g}}, \quad \dot{q}_{1,2} \quad \cdots \quad \dot{q}_{2,\mathrm{g}} \quad \cdots \quad \dot{q}_{m,\mathrm{g}}]^{\mathrm{T}} \tag{4.25}$$

4.3.3 Screw-Based Jacobian Analysis

In this part, the Jacobian matrix of the 3-PSP platform is obtained through the concept of reciprocal screws. Figure 4-4 shows the schematic kinematic chain of a PSP limb where the lower and upper prismatic joints are replaced by $\hat{\$}_1$and $\hat{\$}_5$ and the spherical joint is replaced by three intersecting unit screws, $\hat{\$}_2$, $\hat{\$}_3$and $\hat{\$}_4$.

As previously mentioned, the first Cartesian coordinate system denoted as $O\ (x, y, z)$ is attached to the base platform and the second Cartesian coordinate system denoted as $\acute{O}\ (u, v, w)$ is attached to the moving platform center. The subscript ij denotes joint j =1, 2, 3, 4, 5 on the ith leg. The lower prismatic joints are distributed on the base by an angular position given by the angle α_i which is oriented about the z-axis.

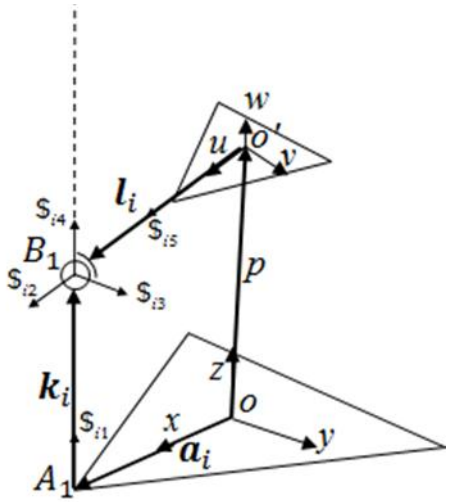

Figure 4-4 : Leg i of the manipulator 3-PSP

There are five joint screws in each limb. The first joint is the sole actuated joint and is an infinite-pitch screw; the four remaining joints are passive joints. If $\mathbf{s}_{ij}$ is the unit vector from the jth joint axis of the ith limb, the five unit joint screws of a limb are as follows:

$$\hat{\$}_{i1} = \begin{bmatrix} \mathbf{0} \\ \mathbf{s_{i1}} \end{bmatrix}, \hat{\$}_{i2} = \begin{bmatrix} \mathbf{s}_{i2} \\ (\boldsymbol{a}_i + \boldsymbol{k}_i) \times \mathbf{s}_{i2} \end{bmatrix},$$
$$\hat{\$}_{i3} = \begin{bmatrix} \mathbf{s}_{i3} \\ (\boldsymbol{a}_i + \boldsymbol{k}_i) \times \mathbf{s}_{i3} \end{bmatrix}, \hat{\$}_{i4} = \begin{bmatrix} \mathbf{s}_{i4} \\ (\boldsymbol{a}_i + \boldsymbol{k}_i) \times \mathbf{s}_{i4} \end{bmatrix}, \text{and } \hat{\$}_{i5} = \begin{bmatrix} \mathbf{0} \\ \mathbf{s}_{i5} \end{bmatrix} \tag{4.26}$$

where

$$\boldsymbol{a}_i = [d\cos\alpha_i \ \ d\sin\alpha_i \ \ 0]^{\mathrm{T}}, \boldsymbol{k}_i = [0 \ \ 0 \ \ q_i]^{\mathrm{T}}, \mathbf{s}_{i5} = [b_x \quad b_y \quad b_z]^{\mathrm{T}} \text{and } \mathbf{s}_{i1} = [0 \quad 0 \quad 1] \tag{4.27}$$

where b_x, b_y and b_z represent the vector $\boldsymbol{l}_i$ components on the x, y and z-axes. The following equation expresses this unit vector in frame B.

$$\begin{bmatrix} b_x \\ b_y \\ b_z \end{bmatrix} = \boldsymbol{Q}.[\cos\alpha_i \quad \sin\alpha_i \quad 0] = \begin{bmatrix} u_x & v_x & w_x \\ u_y & v_y & w_y \\ u_z & v_z & w_z \end{bmatrix}.[\cos\alpha_i \quad \sin\alpha_i \quad 0] = \begin{bmatrix} u_x\cos\alpha_i + v_x\sin\alpha_i \\ u_y\cos\alpha_i + v_y\sin\alpha_i \\ u_z\cos\alpha_i + v_z\sin\alpha_i \end{bmatrix} \quad (4.28)$$

Consider that the joint axes $\mathbf{s}_{i1}$, $\mathbf{s}_{i2}$ and $\mathbf{s}_{i3}$ of the 3-PSP mechanism are parallel to the x, y and z-axes respectively. Therefore the three axes can be written as:

$$\mathbf{s}_{i2} = [1 \quad 0 \quad 0]^{\mathrm{T}}, \mathbf{s}_{i3} = [0 \quad 1 \quad 0]^{\mathrm{T}}, \mathbf{s}_{i4} = [0 \quad 0 \quad 1]^{\mathrm{T}} \quad (4.29)$$

By substituting the eq.(4.27) and (4.28) with eq.(4.26) and taking across product, the screw set $\hat{\$}_i$ can be obtained:

$$\hat{\$}_i = \begin{Bmatrix} \hat{\$}_{i1} = [0,0,0\,,0,0,1]^{\mathrm{T}} \\ \hat{\$}_{i2} = [1,0,0\,,0,q_i,-d\sin\alpha_i]^{\mathrm{T}} \\ \hat{\$}_{i3} = [0,1,0\,,-q_i,0,d\cos\alpha_i]^{\mathrm{T}} \\ \hat{\$}_{i4} = [0,0,1\,,d\sin\alpha_i,-d\cos\alpha_i,0]^{\mathrm{T}} \\ \hat{\$}_{i5} = [0,0,0\,,b_x,b_y,b_z]^{\mathrm{T}} \end{Bmatrix} \quad (4.30)$$

For each leg $\hat{\$}_1$, $\hat{\$}_2$, $\hat{\$}_3$, the screws can be written as:

$$\hat{\$}_1 = \begin{Bmatrix} \hat{\$}_{11} = [0,0,0\,,0,0,1]^{\mathrm{T}} \\ \hat{\$}_{12} = [1,0,0\,,0,q_1,-d]^{\mathrm{T}} \\ \hat{\$}_{13} = [0,1,0\,,-q_i,0,d]^{\mathrm{T}} \\ \hat{\$}_{14} = [0,0,1\,,0,-d,0]^{\mathrm{T}} \\ \hat{\$}_{15} = [0,0,0\,,u_x,u_y,u_z]^{\mathrm{T}} \end{Bmatrix} \quad (4.31)$$

$$\hat{\$}_2 = \begin{Bmatrix} \hat{\$}_{21} = [0,0,0\,,0,0,1]^{\mathrm{T}} \\ \hat{\$}_{22} = [2,0,0\,,0,2q_2,-\sqrt{3}d]^{\mathrm{T}} \\ \hat{\$}_{23} = [0,2,0\,,-2q_2,0,-d]^{\mathrm{T}} \\ \hat{\$}_{24} = [0,0,2\,,\sqrt{3}d,d,0]^{\mathrm{T}} \\ \hat{\$}_{25} = [0,0,0\,,\sqrt{3}v_x - u_x,\sqrt{3}v_y - u_y,\sqrt{3}v_z - u_z]^{\mathrm{T}} \end{Bmatrix} \quad (4.32)$$

$$\hat{\$}_i = \left\{ \begin{array}{c} \hat{\$}_{31} = [0,0,0\ ,0,0,1]^{\mathrm{T}} \\ \hat{\$}_{32} = \left[2,0,0\ ,0,2q_3,\sqrt{3}d\right]^{\mathrm{T}} \\ \hat{\$}_{33} = [0,2,0\ ,-2q_3,0,-d]^{\mathrm{T}} \\ \hat{\$}_{34} = \left[0,0,2\ ,-\sqrt{3}d,d,0\right]^{\mathrm{T}} \\ \hat{\$}_{35} = \left[0,0,0\ ,\sqrt{3}v_x + u_x, \sqrt{3}v_y + u_y, \sqrt{3}v_z + u_z\right]^{\mathrm{T}} \end{array} \right\} \tag{4.33}$$

By considering each limb as an open loop chain and expressing the instantaneous twist $\$_p$ of the moving platform in terms of the joint screws, we obtain:

$$\$_p = \dot{q}_{i,1}\hat{\$}_{i1} + \dot{\theta}_{i2}\hat{\$}_{i2} + \dot{\theta}_{i3}\hat{\$}_{i3} + \dot{\theta}_{i4}\hat{\$}_{i4} + \dot{l}_{i5}\hat{\$}_{i5}, i = 1, 2, 3 \tag{4.34}$$

where $\dot{q}_{i,1}$and $\dot{l}_{i5}$ are the linear velocities of the lower and upper prismatic joints, respectively, and $\dot{\theta}_{i2}, \dot{\theta}_{i2}$ and $\dot{\theta}_{i4}$ are the passive joint rates.

Since the axes of all unactuated and actuated joints pass through point B_i, a screw that is reciprocal to all screws except $\hat{\$}_{i1}$ intersects point B_i and is perpendicular to the plane containing $\hat{\$}_{i3}$ and $\hat{\$}_{i5}$. It is given by:

$$\hat{\$}_{ri,1} = \begin{bmatrix} \mathbf{s}_{ri,1} \\ (\boldsymbol{a}_i + \boldsymbol{k}_i) \times \mathbf{s}_{ri,1} \end{bmatrix} \tag{4.35}$$

where $\mathbf{s}_{ri,1} = \mathbf{s}_{i,3} \times \mathbf{s}_{i,5} = \begin{bmatrix} -(u_z \cos\alpha_i + v_z \sin\alpha_i \\ 0 \\ u_x \cos\alpha_i + v_x \sin\alpha_i \end{bmatrix}$, $\boldsymbol{a}_i + \boldsymbol{k}_i = [d\cos\alpha_i \quad d\sin\alpha_i \quad q_i]$ and

$$(\boldsymbol{a}_i + \boldsymbol{k}_i) \times \mathbf{s}_{ri,1} = \begin{bmatrix} (d\sin\alpha_i).(u_x\cos\alpha_i + v_x\sin\alpha_i) \\ -d(u_z\cos\alpha_i + v_z\sin\alpha_i) - (d\cos\alpha_i).(u_x\cos\alpha_i + v_x\sin\alpha_i) \\ (d\sin\alpha_i).(u_z\cos\alpha_i + v_z\sin\alpha_i) \end{bmatrix}.$$

Equation.(4.35) for each limb can be written as follows:

$$\hat{\$}_{r1,1} = [-u_z, 0, u_x\ ;\ 0, -du_z - du_x, 0\ ]^{\mathrm{T}}$$

$$\hat{\$}_{r2,1} = \left[1/2u_z - \sqrt{3}/2v_z, 0, \sqrt{3}/2v_x - 1/2u_x\ ;\ 3/4v_x - d\sqrt{3}/4u_x, 1/2(du_z - \sqrt{3}v_z, d\sqrt{3}/4(\sqrt{3}v_z - u_z)\right]^{\mathrm{T}}$$

$$\hat{\$}_{r3,1} = \left[1/2u_z + \sqrt{3}/2v_z, 0, -1/2u_x - \sqrt{3}/2v_x\ ;\ 3/4v_x - d\sqrt{3}/4u_x, 1/2(u_z + \sqrt{3}v_z) - 1/4d(u_x - \sqrt{3}v_x\ , d\sqrt{3}/4(\sqrt{3}v_z + u_z)\right]^{\mathrm{T}}$$

By taking the orthogonal product of both sides of eq.(4.34) with (4.35), the result can be written in the matrix form:

$$\left[((\boldsymbol{a}_i + \boldsymbol{k}_i) \times \mathbf{s}_{ri,1})^{\mathrm{T}} \mathbf{s}_{ri,1}{}^{\mathrm{T}}\right] \begin{bmatrix} \boldsymbol{\omega_p} \\ \mathbf{v_p} \end{bmatrix} = [u_x \cos\alpha_i + v_x \sin\alpha_i \quad 0] \tag{4.36}$$

Writing eq.(4.36) three times for each limb, the result is:

$$\mathbf{J}_x \dot{\boldsymbol{x}} = \mathbf{J}_q \dot{\boldsymbol{q}} \tag{4.37}$$

where

$$\mathbf{J}_x = \begin{bmatrix} \left((\boldsymbol{a}_1 + \boldsymbol{k}_1) \times \mathbf{s}_{r1,1}\right)^{\mathrm{T}} & \mathbf{s}_{r1,1}{}^{\mathrm{T}} \\ \left((\boldsymbol{a}_2 + \boldsymbol{k}_2) \times \mathbf{s}_{r2,1}\right)^{\mathrm{T}} & \mathbf{s}_{r2,1}{}^{\mathrm{T}} \\ \left((\boldsymbol{a}_3 + \boldsymbol{k}_3) \times \mathbf{s}_{r3,1}\right)^{\mathrm{T}} & \mathbf{s}_{r3,1}{}^{\mathrm{T}} \end{bmatrix} \tag{4.38}$$

$$\mathbf{J}_q = \begin{bmatrix} u_x \cos\alpha_1 + v_x \sin\alpha_1 & 0 & 0 \\ 0 & u_x \cos\alpha_2 + v_x \sin\alpha_2 & 0 \\ 0 & 0 & u_x \cos\alpha_3 + v_x \sin\alpha_3 \end{bmatrix} \tag{4.39}$$

$$\dot{\boldsymbol{x}} = [\omega_x \quad \omega_y \quad 0 \quad 0 \quad 0 \quad \dot{z}]^{\mathrm{T}} \tag{4.40}$$

$$\dot{\boldsymbol{q}} = [\dot{\mathrm{q}}_1 \quad \dot{\mathrm{q}}_2 \quad \dot{\mathrm{q}}_3]^{\mathrm{T}} \tag{4.41}$$

Equation (4.37) shows the relationship between the instantaneous twist (displacement and rotational velocities of the platform) and the actuated joint velocities. In this equation, $\mathbf{J}_x$ and $\mathbf{J}_q$ are the parallel and serial Jacobian matrices, and $\dot{\boldsymbol{x}}$ and $\dot{\boldsymbol{q}}$ are the instantaneous twist of the platform and the joint velocity, respectively, where ω_x, ω_y, and $\dot{z}$ are the rotational and displacement velocities of the moving platform.

We have presented the basic equations for this mechanism. Theses equations can be used for the analysis of the mechanism such as working space analysis, singularity analysis, dexterity analysis and optimal dimensional analysis.

CONCLUSION

In this thesis a new mechanical design for machining of curved panels, without requiring precise information about the geometry of the surface was presented.

For this purpose, we designed a new passive spatial parallel 3-DOF mechanism which can be mounted on a wrist of robot and perform the machining.

In chapter 2, we introduced a large family of 3-DOF mechanisms. The parallel mechanisms with 3-DOF are suitable for machining that require high stiffness and high payload-to-weight ratio. In addition, we introduced three subgroups of 3-DOF spatial parallel mechanism, which include translation, orientation, and mixed degrees of freedom mechanisms. The zero-torsion spatial 3-DOF parallel mechanisms which have two orientations and one translation degree of freedom are presented. From this group, we chose the 3-PSP mechanism in order to complete our design given that the 3-PSP system orients the cutting tool over the surface so that the cutting tool is always normal to the surface.

In chapter 4, a passive mechanism for machining purposes has been presented. The mechanism is designed so that, it is passive and can, therefore, be mounted on a wrist of a robot and be used for the machining of curved panels without requiring the precise information of the geometry of the surface.

For the orientation of the cutting tool over the surface, the 3-PSP spatial mechanism has been chosen, thus providing the cutting tool with two orientations and one translation degree of freedom.

In order to keep the contact between surface and cutting tool, we designed three sliding pads and to adjust the depth of cut a supplementary system has been designed.

The position analysis of the mechanism was done using the Tilt-and-Torsion Angles, where the position of the prismatic joints has been written as equations of the three variables $\emptyset$, θ and z, so that, the cutting tool may move with 1-DOF translational and 2-DOF orientation motion. Lastly, we used the theory of reciprocal screws for the Jacobian analysis.

REFERENCES

[1] Martinez, M. T. (1992). Machine tool installation for supporting and machining workpiece. US Patent 5, 163, 793.

[2] Hamann, J.-C. (2007). Process and device for machining by windowing of non-deformable thin panels. US Patent 7, 168, 898 B2.

[3] Hamann, J.-C. (2009). Process and mechanical device for machining flexible panels, in particular with a complex shape. US Patent 7, 507, 059 B2.

[4] Panczuk, R., & Foissac, P.-Y. (2010). Process and device for machining of panels. US Patent 7, 682, 112 B2.

[5] Gregorio, R. D. (2003). Inverse position analysis, workspace determination and position synthesis of parallel manipulators with 3-RSR topology. Robotica, 21, 627-632.

[6] Tsai, L.-W. (1999). The Mechanics of Serial and Parallel Manipulators In *Robot Analysis,* John Wiley and Sons: New York, pp.54-168

[7] Merlet, J.-P. (2006). Structural Synthesis and Architectures In *Parallel Robots*, Springer: Dordrecht, Netherlands. pp. 19-94.

[8] Tsai, L.-W. (1998). Systematic enumeration of parallel manipulators. Technical Research Report, 1-12.

[9] Gregorio, R. D. (2001). Kinematics of a new spherical parallel manipulator with three equal legs: the 3-URC wrist. Journal of Robotic Systems, 18 (5), 213-219.

[10] Gregorio, R. D. (2001). A new parallel wrist using only revolute pairs: the 3-RUU wrist.Robotica, 19, 305-309.

[11] Gregorio, R. D. (2002). A new family of spherical parallel manipulators.Robotica, 20, 353-358.

[12] Fang Y., &Tsai, L.-W. (2004). Structure synthesis of a class of 3-DOF rotational parallel manipulators. IEEE Transactions on Robotics and Automation, 20 (1), 117-121.

[13] Bonev, I. A. (2002). Geometric analysis of parallel mechanisms.Doctoral thesis, Université Laval, Québec, Canada.

[14] Pond, G., &Carretero, J. A. (2009). Architecture 0ptimisation of three 3-PRS variants for parallel kinematic machining.Robotics and Computer-Integrated Manufacturing. 25, 64-72.

[15] Carretero, J. A., Podhorodeski, R. P., Nahon, M. A., & Gosselin, C. M. (2000). Kinematic analysis and optimization of a new three degree-of-freedom spatial parallel manipulator. Journal of Mechanical Design. 122, 17-24.

[16] Tsai, M.-S., Shiau, T.-N., Tsai Y.-J., & Chang, T.-H. (2003). Direct kinematic analysis of a 3-PRS parallel mechanism. Mechanism and Machine Theory. 38, 71-83.

[17] Merlet, J.-P. (2001). Micro parallel robot MIPS for medical applications. IEEE. 2, 611-619.

[18] Liu, X.-J., Wang, L.-P. Xie, F. &Bonev, I. A. (2010). Design of a three-axis articulated tool head with parallel kinematics achieving desired motion/force transmission characteristics. Journal of Manufacturing Science and Engineering.132 (2), ISSN 1087-1357.

[19] Myszka, D. H. (2005). Multidegree of Freedom Linkages In *Mechanics of Machines* .Wiley: New York. pp. 85-116

[20] Doughty, S. (1988).Introduction to Mechanisms and Kinematics In *Machines & Mechanisms* . Pearson Education: New Jersey. pp.1-41

[21] Bonev, I. A., ''ParalleMic-the Parallel Mechanisms Information Center'', IlianBonev, 2000-2007, http://www.parallemic.org/.

[22] Tsai, L.-W., & Stamper, R. E. (1997). A parallele manipulator with only translational degrees of freedom. Technical Research Report. 1-18.

[23] Qi, H., Liwen, G., Jinsong, W., & Liping, W. (2009). Dynamic freeforward control of a novel 3-PSP 3-DOF parallel manipulator. Chinese Journal of Mechanical Engineering. DOI: 10.3901/CJME.2009.03.